Master thesis

Université de Liège - GIGA Neurosciences
Laboratory of the Molecular Regulation of Neurogenesis

Dacapo regulates axonal transport through the modulation of microtubule acetylation

A master's thesis submitted in fulfillement of the requirements for the degree of Master in Biomedical Sciences

Author
Romain Le Bail

Supervisors
Giovanni Morelli
Ivan Gladwyn-Ng

Promoter
Laurent Nguyen

2016-2017

Acknowledgments

I would like to express my sincere gratitude to Laurent Nguyen gave me the opportunity to work in this welcoming, enriching and warm environment and for that I am greatly thankful. His precious input on the structure of the manuscript were extremely helpful and I am looking forward to pursuing my journey in his lab

Loads of gratefulness to Giovanni Morelli and Ivan Gladwyn-Ng for their relentless supervision over the course of my master's thesis. Our many talks and your diligent reading of the manuscript were enlightening and taught me more than I could have hoped for. Thank you for all the time and effort you've dedicated to my technical and scientific formation with such a casual and friendly attitude. Ivan, our informal talks about astrophysics, philosophy, theology (you too Chris !), history, management were eye and mind opening. Giovanni, thank you for your constant input on how to be a better researcher but most of all thank you for making me feel like a PhD pokemon trainer !

Over the course of my master's thesis, I've had the opportunity to meet many interesting and kind hearted people. I would like to give my warm appreciation to Sébastien, Gulistan, Céline, Sophie, Laura, Ron, Fanny for the many fun and relaxing coffee breaks but also all the memorable random chats or singalongs that made these few months some of the best of my life. Special dedication to Senseibastien for his friendship and support at all times, I may have lost some bets but at least I have not lost my will !

Very warm thanks to the Nguyen and Malgrange groups as a whole for their technical and intellectual help throughout the master. In addition to that, you made the work environment feel like home with the barbecues, squash games and your general enthousiasm. I cannot thank all of you enough for making this enriching experience a fun and thrilling adventure !

Enormous thanks to my office mates Vincent, Sonia and Marine. You have made the office a cheerful place but also a temple of statistics to which I was lucky enough to be initiated. My philosophical discussions with Sonia, although not academic, were also profitable and I hope we can come to a conclusion as to the meaning of life at some point !

U are all the very best, like no one ever was !

Abstract

Neurons are highly polarized cells with a long axon extending from the soma to reach distant targets. The axon carries action potentials that convey signals to distant cells by releasing neurotransmitters at the synapse. This synaptic input is at the foundation of neurotransmission but requires constant energy and protein supply. The axon and synapses therefore rely on the synthetic and recycling abilities of the cell-soma as well as on an active transport system called axonal transport. Anterograde transport ensures the delivery of newly synthesized proteins, lipids, RNA and organelles from the cell soma to the axon to maintain pre-synaptic activity. Conversely, retrograde transport removes aging proteins and organelles from the distal axon while delivering neurotrophic signals to the cell-soma. Cargos are driven in both directions but are also directed to specific sub-cellular compartments by cargo-specific mechanisms of regulation that rely on the diversity among microtubule tracks, motors or scaffolding proteins.

$p27^{kip1}$ was originally discovered as a cell-cycle inhibitor and then emerged as a multifunctional protein with roles extending beyond cell-cycle regulation such as microtubule binding, promotion of microtubule polymerization and regulation of microtubule acetylation. These non-canonical functions of $p27^{kip1}$ led to the hypothesis that this protein could be involved in the regulation of axonal transport. *Drosophila Melanogaster* is a prime model for the investigation of axonal transport and we therefore studied the mechanisms regulating axonal transport by focusing on dacapo, the *drosophila* ortholog of $p27^{kip1}$. We show that dacapo depleted larval motoneurons display anterograde and retrograde slowdown in the velocity of mitochondria and synaptic vesicles, concomitant with a reduction of microtubule acetylation levels. Although no synaptic morphological defect was highlighted at the neuromuscular junction, dacapo knockdown animals exhibited locomotor behavior defects at the larval and adult stage. Restoring physiological tubulin acetylation with a histone deacetylase 6 (HDAC6) inhibitor subsequently ameliorated the transport velocity of mitochondria and synaptic vesicles and rescued the motor defects. Together our results highlight dacapo as a regulator of microtubule acetylation which subsequently modulates the transport velocity of mitochondria and synaptic vesicles along microtubules. The rescue of locomotor behavior defects by HDAC6 inhibition suggests that physiological axonal transport may be required to ensure proper synaptic function in dacapo knockdown larvae, independently of synaptic morphology changes.

Résumé

Les neurones sont des cellules fortement polarisées de par leur axone qui s'étend depuis le soma afin d'atteindre des cibles distantes. L'axone conduit les potentiels d'actions qui transmettent les signaux en libérant des neurotransmetteurs à la synapse. Ce mode de signalisation constitue le fondement de la neurotransmission mais requiert un ravitaillement constant d'énergie et de protéines. L'axone et les synapses dépendent donc de la capacité du soma à synthétiser des protéines et à les recycler mais aussi d'un système de transport actif appelé transport axonal. Le transport antérograde assure la distribution de protéines néo-synthétisées, de lipides, d'ARN et d'organelles depuis le soma jusqu'à l'axone afin de maintenir l'activité pré-synaptique. A l'inverse, le transport rétrograde élimine les protéines et organelles vieillissant tout en délivrant au soma des signaux neurotrophiques. Les cargos transitent dans les deux directions mais sont aussi dirigés vers des sous compartiments cellulaires par des mécanismes de régulation spécifiques aux cargos qui reposent sur la diversité que montrent les microtubules, les moteurs ou les protéines d'échafaudage.

$p27^{kip1}$ a été décrite comme un inhibiteur du cycle cellulaire mais est maintenant considérée comme une protéine multifonctionnelle avec des rôles tels que la fixation aux microtubules, leur acétylation ou la promotion de leur polymérisation. Ces fonctions non-canoniques de $p27^{kip1}$ ont mené à l'hypothèse que cette protéine pourrait être impliquée dans la régulation du transport axonal. *Drosophila Melanogaster* est un modèle de choix pour l'investigation du transport axonal et par conséquent nous avons étudié les mécanismes régulant le transport en se focalisant sur dacapo, l'orthologue de $p27^{kip1}$ chez la drosophile. Nous montrons que la déplétion de dacapo dans les motoneurons de larve entraîne une diminution de la vélocité antérograde et rétrograde des mitochondries et vésicules synaptiques, concomitante avec une réduction des niveaux d'acétylation des microtubules. Bien qu'aucun défaut morphologique n'ait été mis en évidence à la jonction neuromusculaire, les animaux déplétés en dacapo présentaient des déficits locomoteurs au stade de larve et d'adulte. La restauration d'une acétylation physiologique par un inhibiteur d'histone désacétylase 6 (HDAC6) augmentait la vélocité des mitochondries et vésicules synaptiques tout en restaurant la locomotion. Nos résultats impliquent dacapo dans la régulation de l'acétylation des microtubules, laquelle module la vélocité des mitochondries et vésicules synaptiques. La restauration des déficits locomoteurs par l'inhibition d'HDAC6 suggère qu'un transport axonal physiologique puisse être nécessaire pour assurer la fonction synaptique chez les larves déplétées en dacapo, et ce indépendamment de changement morphologiques à la synapse.

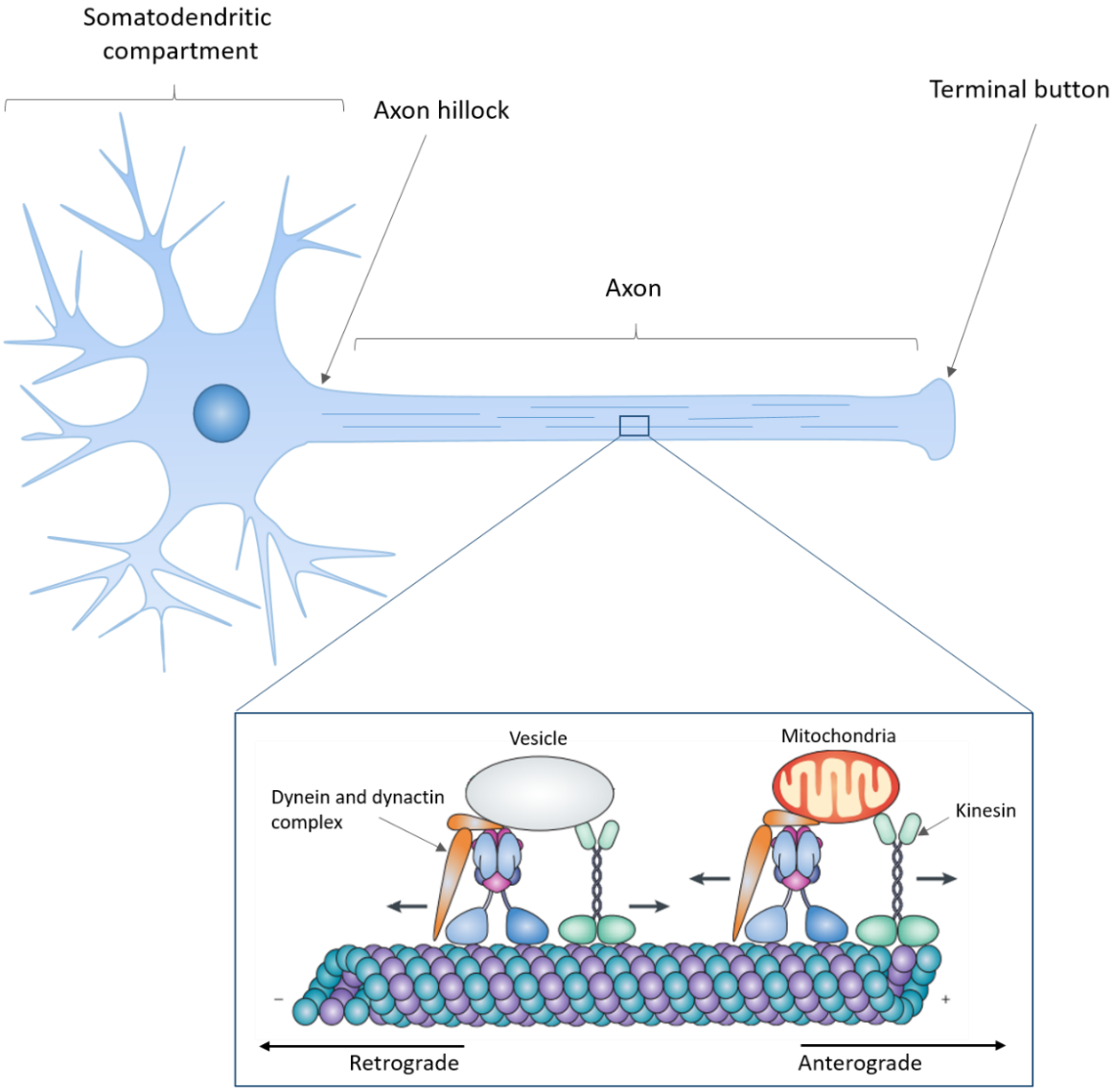

Figure 1.1: Axonal transport overview (adapted from Millecamps & Julien 2013)
Neurons are polarized cells with a dendritic arborescence and a single long axon emerging from the cell body. Microtubule tracks are distributed along the axon to support the transport of various cargos such mitochondria or proteins contained in vesicles. Anterograde transport refers to the delivery of cargos towards the axon termination which is powered by kinesin motors. Conversely, cargos transported towards the cell soma are propelled by cytoplasmic dynein in a process termed retrograde transport.

1. Introduction

Neurons are highly polarized cells due to their extended neurites emerging from the cell body. Dendrites emerge in a treelike fashion to receive inputs from other neurons while the axon extends over long distances to convey electrical signals generated at the axon hillock. The conduction of the axon potential and release of neurotransmitters at the synapse requires constant energy and protein supply. However, protein synthesis is restricted to the cell soma and dendrites while the axon lacks the required machinery for its high protein demands. The axon therefore relies on the synthetic abilities of the cell soma and the constant supply of these proteins by active transport, a process called axonal transport. Human motoneurons can have axons extending as far as one meter away from the cell body, highlighting the challenge that axonal transport must overcome (Twelvetrees et al., 2012).

The materials transported along the microtubule cytoskeleton are named cargos. They are propelled by kinesins and dynein motors that drive bidirectional axonal transport. Kinesins transport cargos in an anterograde manner, from the cell soma to the axon terminations to ensure the delivery of newly synthesized proteins, lipids, RNA and organelles to the axon. Conversely the retrograde movement of cargos from the axon to the cell body is mediated by dynein and is required for the degradation and recycling of these components (Twelvetrees et al., 2012). For their part, mitochondria are transported both in an anterograde and retrograde manner to adjust to energy demands (Saxton and Hollenbeck, 2012) (Figure 1.1).

Our current understanding of axonal transport supports a model in which heterogeneous cargo-specific patterns of motility ensures delivery in the destined sub-cellular compartments (Maday et al., 2014). This heterogeneity in the transport patterns and spatial delivery of cargos emerges from the diversity and fine tuning of motors, microtubules and cargos. One of the putative mechanism regulating the movement of cargos is microtubule acetylation. This post-translational modification of microtubules has been widely studied in the recent years (reviewed in Li and Yang, 2015; Sadoul and Khochbin, 2016). Although its functions remain elusive, promising studies suggest that acetylated microtubules modulate the speed and spatial delivery of the cargos they support in mammal embryonic primary cultures and *drosophila* larvae (Reed et al., 2006; Dompierre et al., 2007; Godena et al., 2014). Hence, I will summarize the current literature regarding axonal transport, with emphasis on the heterogeneity of the key players. I will then focus on microtubule acetylation and its role in the regulation of axonal transport, linking this post-translational modification to $p27^{kip1}$, termed hereafter p27. Finally, I will introduce *Drosophila Melanogaster* as a model for physiological and biomolecular studies as well as axonal transport.

1.1 The regulation of axonal transport involves heterogenic molecular motors

The motility patterns of axonal transport can be subdivided in two main categories: slow axonal transport (reviewed in Roy, 2013) and fast axonal transport (reviewed in Maday et al., 2014). Organelles such as mitochondria or vesicles loaded with proteins are transported at fast speeds of about 400mm/day or ~ 4µm/s (Griffin et al., 1976). On the other hand, soluble proteins and neurofilament polymers are slowly transported at speeds averaging 1-10mm/day or ~ 1-10µm/s (Griffin et al., 1976). Slow axonal transport appears responsible for the trafficking of approximately three quarters of the proteins reaching synapses (Garner and Lasek, 1982; Roy, 2013). Nonetheless, the mechanisms of fast axonal transport have been extensively studied whereas slow axonal transport remains more enigmatic due to the difficulty in visualizing slow moving particles.

Breakthroughs in the field of confocal microscopy and molecular biology enabled the identification of more types of cargos and patterns of motility among fast moving organelles. Diverse cargos are transported in a compartment specific manner and at different speeds to meet specific cellular demands. This heterogeneity in motility patterns is thought to result from cargo-specific mechanisms of regulation reviewed in Maday et al., 2014. Motors but also to some extent microtubule tracks may be unique to their specific cargo. I will introduce these players while providing examples that illustrate how the diversity they display contributes to cargo-specific regulation.

1.1.1 The kinesin superfamily

Molecular motors consume ATP to actively drag cargos along the microtubule tracks. Kinesin-1, was the first protein that exhibited such properties (Vale et al., 1985) and has been determined as a driver of anterograde transport (Hirokawa et al., 1991). Later on, the microtubule-associated motor dynein was discovered (Paschal, 1987) and implicated in retrograde transport (Paschal and Vallee, 1987). Based on a database search of the human and mouse genome, 45 different kinesins have now been identified among which 38 are expressed in the mouse brain across all developmental stages (Miki et al., 2001). The expression of 20 different kinesins has also been highlighted in mature mouse hippocampal neurons cultured *in vitro*, illustrating the diversity of anterograde motors in neurons (Silverman et al., 2010).

Some kinesin isotypes are associated with specific cargos, which suggests cargo-specific mechanisms of transport mediated by kinesin isotypes. For instance, KIF1A, a member of the kinesin-3 family, is implicated in the transport of dense core vesicles destined to synapses (Lo et al., 2011). In the same study, Lo et al. showed that the transport of mitochondria is unaffected by the knockdown of KIF1A. Instead mitochondria transport relies mostly on KIF5A (Campbell

et al., 2014), KIF5B (Tanaka et al., 1998) and KIF5C (Kanai et al., 2000) of the kinesin-1 family and partially on KIF1Bα of the kinesin-3 family (Lo et al., 2011; Okada et al., 1995). Together these studies show that almost all kinesin isotypes are expressed in the brain across developmental stages but a wide diversity of kinesins are also expressed in a homogenous neuronal population. This particularity of nerve cells may reflect the need for a fine tuning of axonal transport, partially achieved by the cargo-specific binding of kinesin motors.

1.1.2 Cytoplasmic dynein complexes

Dynein is the motor driving retrograde transport and its function requires the dynein activator dynactin, a highly conserved multiprotein (Schroer, 2004). Dynactin binds to dynein and microtubules to initiate retrograde transport at the distal ends of microtubules (Moughamian and Holzbaur, 2012). Dynein itself is a complex for which the heavy chain provides the ATPase activity and binds to microtubules. The heavy chain of cytoplasmic dynein is encoded by a single gene and therefore, retrograde axonal transport relies exclusively on the heavy chain of cytoplasmic dynein to drive cargos towards the cell soma (Pfister, 2015). In addition to its role as the generator of stall force, the heavy chain of the dynein complex acts as a scaffold for the other subunits. The intermediate chain, the light intermediate chain and the three light chains bind together with two heavy chains to form the dynein complex (Trokter et al., 2012). While the heavy chain is encoded by a single gene, the other subunits display genomic diversity and all heterodimers combinations can be generated in vitro (Lo et al., 2006). The subunit diversity of dynein may thus be at the origin of cargo specific transport. For instance Mitchell et al., 2012 show that IC-2C and IC-2B, two intermediate chain isotypes, co-localize respectively with mitochondria and endosomes in rat cells.

1.2 Microtubules: malleable rails supporting axonal transport

Microtubules serve as tracks for axonal transport but have many other functions including scaffolding for cilia and flagella, chromosome segregation during mitosis, regulation of cell polarity and morphogenesis (Akhmanova and Steinmetz, 2015; Conde and Cáceres, 2009). Their role as the main support for axonal transport was discovered by Schnapp et al. in 1985 and since then, the dynamic nature and diversity of microtubule tracks emerge as modulators of axonal transport.

1.2.1 Microtubule structure and dynamics

Microtubule filaments consist of dimers of α and β tubulin that associate together in a non-covalent and dynamic way (reviewed in Akhmanova and Steinmetz, 2015). In the axon, all microtubules are uniformly polarized with their fast growing +end directed towards the axon

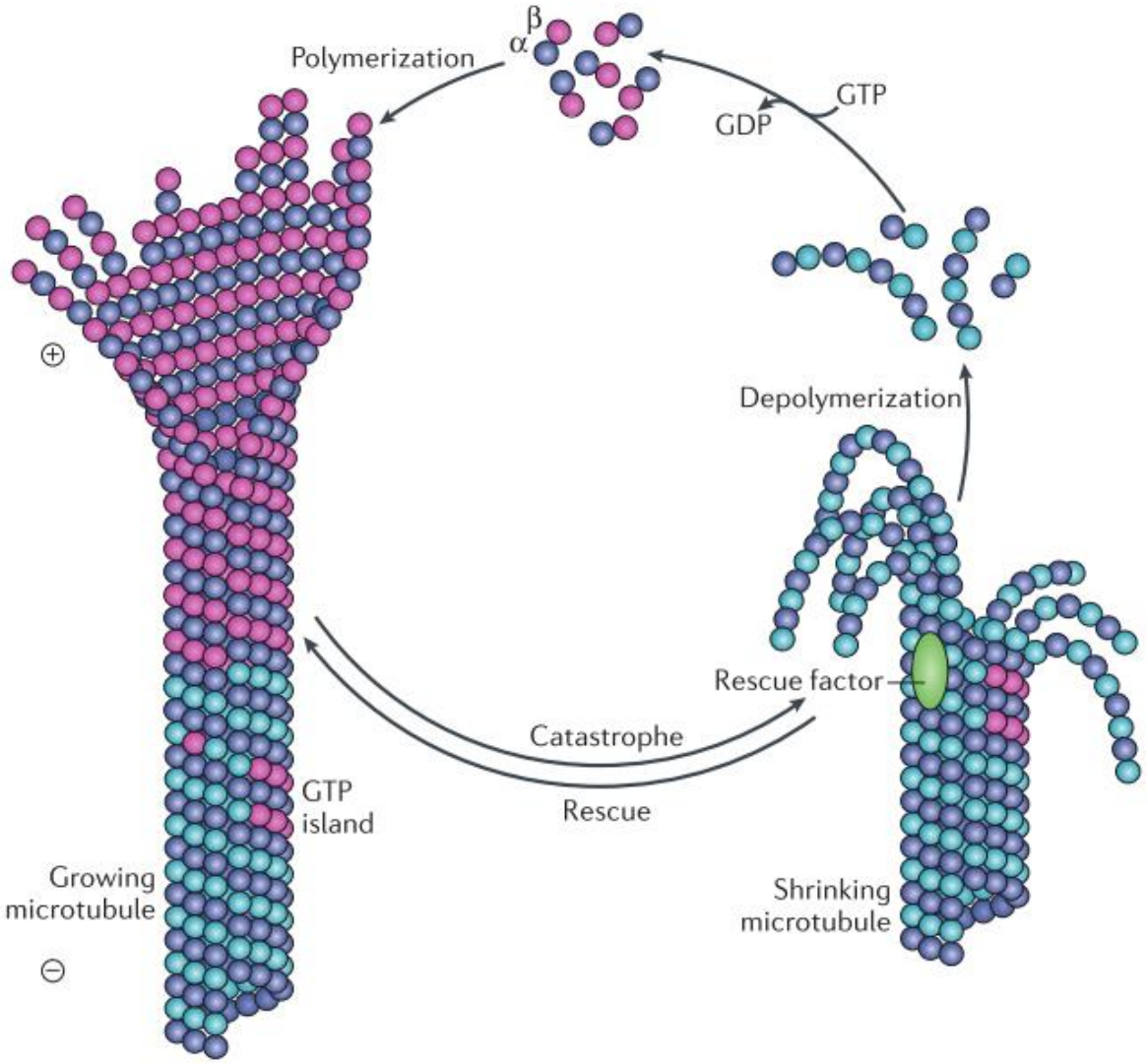

Figure 1.2: Microtubule dynamics (from Akhmanova & Steinmetz 2015)
Microtubules are constituted by dimers of α- and β-tubulin that polymerize predominantly at the + end of microtubules. GTP-bound tubulin dimers are incorporated into growing microtubules and GTP-hydrolysis occurs progressively so that a GTP-cap is maintained at the tip of growing microtubules. Microtubules are stabilized by GTP-bound tubulin whereas GDP-bound tubulin has the opposite effect. The presence of the GTP-cap ensures the stability of the growing microtubule but once the kinetics of GTP-hydrolysis outweighs the incorporation of new tubulin dimers, the GTP-cap is lost and the microtubule lattice becomes unstable. The fast depolymerization of microtubules is termed "catastrophe" and it can be "rescued" by GTP islets or rescue factors. The "rescue" transiently stabilizes microtubules to enable the incorporation of new tubulin dimers and therefore the formation of a new GTP-cap.

terminations (Stepanova et al., 2003). They alternate between phases of polymerization and depolymerization in a cyclic manner, a process termed "dynamic instability", first coined by Mitchison and Kirschner, 1984. In short, GTP-bound β-tubulin stabilizes microtubules whereas GDP-bound β-tubulin changes the conformation of the dimer and induces strain on the microtubule's lattice (Alushin et al., 2014). According to a conceptual model first described in (Carlier and Pantaloni, 1981), growing microtubules display a GTP cap that stabilizes their structure and enables them to grow further. As their length increases, GTP is hydrolyzed into GDP, which affects allosteric protofilaments interactions and destabilizes microtubular structure (Yajima et al., 2012). If the GTP cap is lost, the stability of the + end is compromised and the microtubule is prone to depolymerization. The fast depolymerization of microtubules is termed catastrophe and it can be rescued once the GTP cap is restored (Desai and Mitchison, 1997) (Figure 1.2).

Polymerizing microtubules bind a complex of plus-end interacting proteins or +TIPs which subsequently facilitates the initiation of retrograde transport through dynactin interaction with dynein (Moughamian et al., 2013). The very dynamic nature of microtubules may thus contribute to the regulation of transport in addition to the versatility it confers to these filaments.

1.2.2 Microtubule diversity

Interestingly, wide heterogeneity exists between microtubules due to many different tubulin isotypes (reviewed in Janke, 2014), post-translational modifications (PTMs) on tubulin residues (reviewed in Song and Brady, 2015) and a myriad of microtubule associated proteins (MAPs) (reviewed in Akhmanova and Steinmetz, 2015).

Tubulin isotypes are α- or β-tubulin proteins with small variations in their amino acid sequence that are encoded in a single organism (Ludueuna, 1993). They are found in many species including human and rodents (Little and Seehaus, 1988) but also *drosophila* (Rudolph et al., 1987) and they are expressed in a tissue specific manner. For instance, in vertebrates, while β1 is found in most tissues, β2 is enriched in the brain and β3 is specific to neurons (Sullivan, 1988). In vitro research has shown that different kinesin motor subtypes exhibit different velocities depending on the tubulin isotype composing the microtubule track (Sirajuddin et al., 2014). This supports a model in which microtubule rails each have a "tubulin code" giving specificity to the transport of cargoes.

MAPs constitute a complex interconnected network of proteins that bind to microtubules to exert diverse effects on their dynamic behavior (Akhmanova and Steinmetz, 2015). Some MAPs have been implicated in the regulation of sub-cellular specific delivery. For instance, CLIP-associating protein 2 (CLASP2) is a MAP that promotes the capture of microtubule +

ends at the synaptic membrane. This microtubule network organization subsequently drives the focal delivery of acetylcholine receptors by vesicles transported along the attached microtubule (Basu et al., 2015). Vershinin et al., 2007 also demonstrated a role of MAPs in the regulation of axonal transport *in vitro* by showing that the mainly axonal MAP tau reduces kinesin motors attachment rate. In the presence of tau, kinesin motors deploy less force and are more likely to dissociate from the microtubule.

In addition to tubulin isoforms and MAPs, PTMs of tubulin are emerging as decisive regulators of microtubule properties and function and as a major contributor to microtubules diversity. PTMs are covalent modifications of proteins that broaden the scope of protein functionalities. The most studied microtubule PTMs are detyrosination, glutamylation, glycylation, phosphorylation and acetylation. These modifications modulate microtubule functions and can occur differentially in specific sub-cellular compartments (Janke and Chloë Bulinski, 2011).

Together, tubulin isoforms, MAPs and PTMs define microtubule identities at the tissue and cellular level to adjust microtubule function. As the aim of this master's thesis was to shed light on the regulation of axonal transport by microtubule acetylation, we will now focus on this specific PTM.

1.3 Microtubule acetylation

Although most PTMs occur at the C-terminal domain of tubulins, which extends in the cytoplasm, acetylation occurs on the lysine 40 (Lys40) of α-tubulin. This amino-acid is located inside the lumen of microtubules, making α-tubulin acetylation the only microtubule PTM occurring inside the microtubule lattice (Howes et al., 2014). The degree of microtubule acetylation depends on the balance between acetyltransferase and deacetylase activity. In recent years, the main effectors of acetylation have been identified but their regulation and the biological role of acetylation remains elusive (reviewed in Li and Yang, 2015; Sadoul and Khochbin, 2016).

1.3.1 Tubulin deacetylases and acetyl-transferases

The deacetylation of tubulin is carried out by histone deacetylase 6 (HDAC6) (Hubbert et al., 2002; Zhang et al., 2003) and sirtuin 2 (SIRT2) (North et al., 2003) which act together to reverse Lys40 acetylation on tubulin. Even though HDAC6 and SIRT2 are part of the histone deacetylase family, only SIRT2 has the ability to deacetylate histones (Seidel et al., 2015). SIRT2 is predominantly cytoplasmic but is transported in the nucleus during mitosis to achieve its function as an histone deacetylase (North and Verdin, 2007). On the other hand, HDAC6 is observed in the nucleus of undifferentiated cells but relocates to the cytoplasm after

differentiation for many tissues including the brain (Chen et al., 2013). Both HDAC6 and SIRT2 display multiple functions due to the varied targets they deacetylate such as cortactin and heat shock protein (HSP)90 for HDAC6 or p53 and histone H4 for SIRT2 (reviewed in Harting and Knöll, 2010; Seidel et al., 2015).

The ARD1-NAT1 complex was the first reported microtubule acetylator in purified microtubule fractions (Ohkawa et al., 2008). Studies in mice and *C. Elegans* then described an α-tubulin acetyl-transferase activity by Elp3 of the Elongator complex (Creppe et al., 2009; Solinger et al., 2010a). Next followed the discovery of GCN5 (Conacci-Sorrell et al., 2010), an histone acetyl transferase. Finally, alpha-tubulin N-acetyltransferase 1 (αTAT1) was described as the main acetyl-transferase in mammals (Akella et al., 2010; Kim et al., 2013). αTAT1 is expressed across all tissues in embryonic and adult mice and αTAT1 knockout mice display no detectable microtubule acetylation in the brain (Kim et al., 2013). In *C. Elegans*, the depletion of αTAT1 or its paralog alpha-tubulin N-acetyltransferase 2 (αTAT2) resulted in diminished but detectable levels of microtubule acetylation while double null mutants exhibited no detectable α-tubulin acetylation in whole worm lysates (Shida et al., 2010). These findings indicate that αTAT1 in mammals, or αTAT1 and αTAT2 in *C. Elegans* are the main acetylators of microtubules while Elp3, GCN5 and ARD1-NAT1 may only be responsible for the regulation of tubulin acetylation or minor tubulin acetylation *in vivo*.

1.3.2 Biological functions of tubulin acetylation

The study of microtubule acetylation functions has become more accessible with the discovery of the main enzymes regulating tubulin acetylation levels. It is now possible to manipulate these enzymes to observe the physiological processes underlying microtubule acetylation (reviewed in Li and Yang, 2015; Sadoul and Khochbin, 2016).

Various studies have been carried out on the link between microtubule acetylation and stability with conflicting results that may be due to the diversity of cell types and models that have been used. Microtubules with a high turnover rate tend to be less acetylated than the stable ones in human fibroblasts (Webster and Borisy, 1989) and stable microtubules in the axons display high levels of acetylation (Cambray-Deakin and Burgoyne, 1987). These observations led to the hypothesis that tubulin acetylation stabilizes microtubules. However, non-acetylated stable microtubules or highly acetylated unstable microtubules have been observed in marsupial kidney cells and chick embryo fibroblasts respectively (Schulze et al., 1987). This suggests that microtubule acetylation is not a prerequisite for increased stability. In addition, HL-1 atrial myocytes exhibit a normal response to nocodazole, a drug inducing microtubule depolymerization, notwithstanding that their microtubule network is fully acetylated

(Belmadani et al., 2004). This suggests that even though acetylation is often correlated with aged microtubules in some cell types, there may not be a causative link between acetylation and microtubule stability.

Promising studies have now implicated the degree of α-tubulin acetylation in transport with particular emphasis on neurons. Reed et al., 2006 have demonstrated that microtubule acetylation increases kinesin-1 binding and moving speed. They also show that the cargo protein JNK-interacting protein 1 (JIP1) is transported by kinesin-1 along acetylated microtubule tracks towards a subset of neurite tips. This suggests a contribution of microtubule acetylation to sub-compartment specific delivery as well as a modulation of transport speed. When acetylation of microtubules was upregulated by a pharmacological inhibitor of HDAC6, the entire microtubule network exhibits high levels of acetylation and JIP1 then accumulates in all neurite tips (Reed et al., 2006). This remarkable observation suggests that only a subset of microtubules may be acetylated in the dendrites of hippocampal neurons thus serving as rails driving specific cargos to their destined subcellular spaces. In a model of Huntington's disease, Dompierre et al., 2007 have shown that HDAC6 inhibition increases microtubule acetylation and subsequently increases the speed of vesicular transport. In a similar study conducted in a *drosophila* model of Parkinson's disease, Godena et al., 2014 have shown that mutant leucine-rich repeat kinase 2 (LRRK2) interacted with deacetylated microtubules to inhibit axonal transport. Following upregulation of microtubule acetylation by HDAC6 inhibitors or αTAT1 overexpression, the affinity of LRRK2 for microtubules was diminished and the transport defect was rescued. Finally, HDAC6 inhibitors have also been used to rescue axonal transport defects in a mouse model of Charcot-Marie-Tooth disease (d'Ydewalle et al., 2011). This treatment remarkably rescued the locomotor behavior of the mutant mice, suggesting that rescuing axonal transport by increasing microtubule acetylation may be a putative therapeutic strategy for some neurodegenerative diseases (Millecamps and Julien, 2013). Taken together, these studies strongly suggest that microtubule acetylation may act to regulate the speed of intracellular trafficking but also the specificity of cargo transport through differential acetylation in the microtubule network of a single neuron.

1.4 Dacapo/p27^{kip1} may be involved in the regulation of axonal transport

The fine tuning of transport requires intricate molecular pathways that remain to be comprehensively understood. Studying the upstream regulators of transport such as the ones orchestrating microtubule acetylation would enable a broader understanding of axonal transport and promote the discovery of pharmacological targets to modulate transport in disease states.

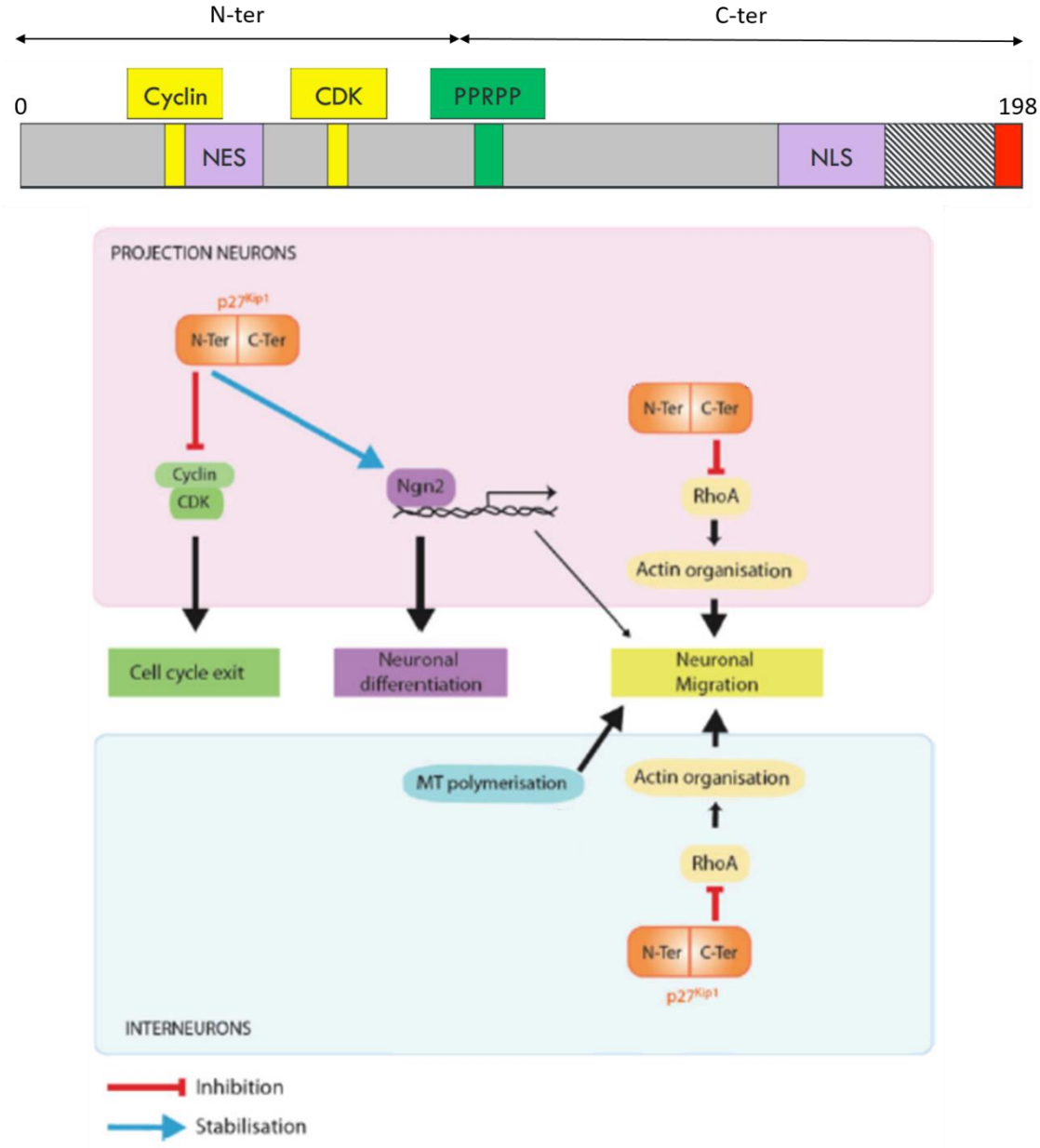

Figure 1.3: p27^{kip1} is an intrinsically disordered multifunctional protein (Adapted from (Godin & Nguyen 2014))

A) p27 is an intrinsically disordered protein without a fixed three dimensional structure. p27 binds multiple targets through specific domains which subsequently induces the folding required to exert its function. The C-terminal part interacts with various proteins and bears the proline-rich domain necessary for p27 microtubule-associated function but not the ability to bind microtubules. Instead p27 appears to bind microtubules through both the N and C-terminal. The cell-cycle related functions of p27 rely on the N-terminal where the cyclin-dependent kinase (CDK) and cyclin binding sites are localized. The N-terminal part is also necessary for the stabilization of Neurogenin-2 (Ngn2) by p27, an activity that does not require the CDK and cyclin binding sites. To regulate the shuttling of p27 between the nucleus and cytoplasm, a putative nuclear localization signal (NLS) and nuclear export signal (NES) have been identified.

B) Multiple functions of p27 have been unraveled in the context of corticogenesis. The canonical function of p27 is to promote cell-cycle exit by associating with CDK/cyclin complexes to prevent G1-S phase transition. Independently from its cell-cycle dependent activities, p27 is able to regulate neuronal differentiation by stabilizing Ngn2, a proneuronal transcription factor. p27 also promotes neuronal migration in both interneurons and projection neurons by interacting with proteins involved in cytoskeleton remodeling. In interneurons and projection neurons, p27 inhibits RhoA leading to a reorganization of the actin cytoskeleton that is required to ensure the proper migration. In interneurons specifically, p27 controls migration by binding to microtubules and promoting their polymerization.

With this in mind, we aim to shed light on dacapo, the D*rosophila Melanogaster* homolog of $p27^{kip1}$, hereafter named p27.

1.4.1 Dacapo/p27 regulate the cell cycle

p27 is a protein of the Cip/Kip family originally discovered as a cell cycle regulator (Toyoshima and Hunter, 1994). It inhibits the G1/S phase transition by regulating a broad range of cyclin-dependent kinases (CDKs) using its conserved CDK-inhibitory domain in the N-terminal (Lacy et al., 2004). Multiple cancers display mutations in p27 due to its role in cell cycle regulation, which justifies the large body of research related to p27 relation with cancer (Bencivenga et al., 2017).

In *drosophila*, the literature has mostly focused on dacapo as a cell cycle regulator that inhibits cyclin E/cdk2 complexes to arrest the G1 phase at a specific developmental stage (Lane et al., 1996). During the *drosophila* brain development, dacapo is specifically upregulated in postmitotic cells called ganglion cells to stop their proliferation (Colonques et al., 2011).

1.4.2 p27 is a multifunctional protein with cell-cycle independent functions

Proteins of the Cip/Kip family have now emerged as multifunctional proteins with cell cycle-independent functions such as transcriptional regulation, cell migration, cell fate determination or cytoskeletal dynamics (Besson et al., 2008). To our knowledge, non-canonical functions of dacapo have not yet been demonstrated in flies. However, the homology in the amino acid sequence of p27 and dacapo suggests a putative functional homology. p27 exerts its many functions by virtue of its intrinsically disordered nature (Bienkiewicz et al., 2002; Wang et al., 2011) (Figure 1.3A). This protein and the Cip/Kip paralogs lack a secondary or tertiary structure in physiological conditions. Instead they bind to their many targets through specific domains which subsequently induces the folding of the protein responsible for its activity (Yoon et al., 2012).

Non-canonical functions of p27 have been studied in the brain where this protein has been linked to the control of neuronal differentiation and migration during cortical development (reviewed in Godin and Nguyen, 2014) (Figure 1.3B). Cortical development involves a tight regulation of neuronal differentiation and migration by transcriptional programs and molecular signaling pathways. In mice, the genesis of the cortical layers occurs between E11 and E18 (Gupta et al., 2002). p27 is expressed throughout the developing mouse cortex, both in progenitors and postmitotic neurons (Itoh et al., 2007). The N-terminal of p27 has been shown to stabilize the transcription factor Neurogenin-2, crucial to trigger the switch between the progenitor and the neuronal state (Nguyen et al., 2006). Also, the C-terminal tail of p27 promotes neuronal migration in interneurons and projection neurons through a cooperative

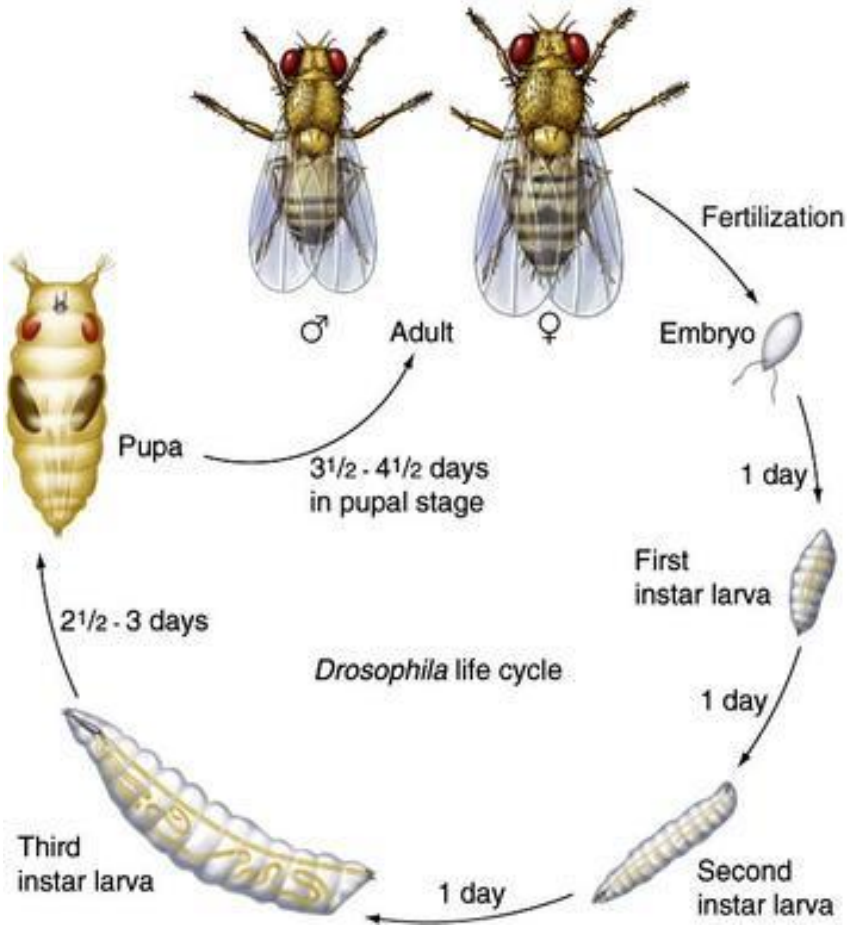

Figure 1.4: Life cycle of the Drosophila Melanogaster (From http://www.creative-diagnostics.com/)
The life cycle of the drosophila comprises four stages: egg, larva, pupa and fly. 8 hours after eclosion, female adults will mate and shortly after they will lay eggs that hatch in a day. The larval stage lasts for an average of 5 days during which larvae pass through the stages of 1st instar, 2nd instar and 3rd instar. Once larval development is complete, animals metamorphose within a pupal case over the course of approximately 4 days. Adult flies then emerge from the case in a process termed eclosion thus allowing the cycle to repeat itself.

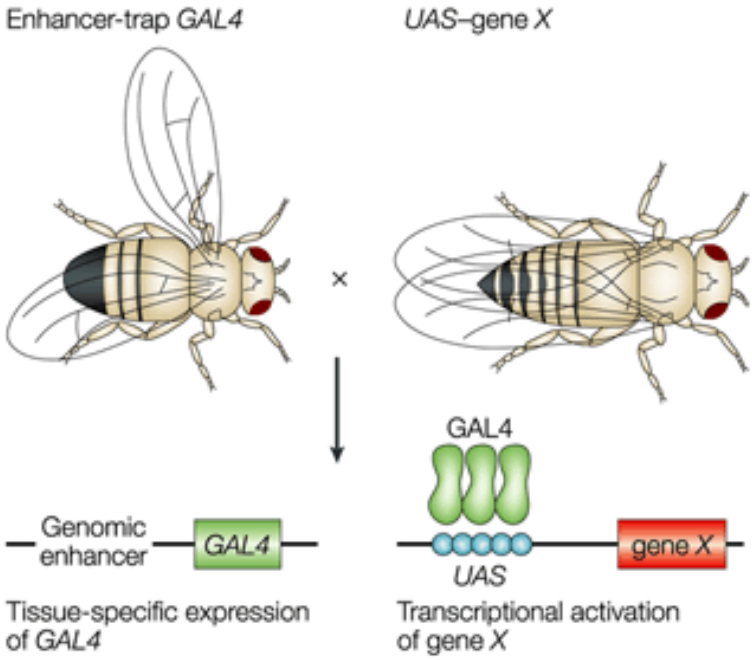

Figure 1.5: The GAL4/UAS system (from St Johnston 2002)
The GAL4/UAS system is a regulator of transcription in yeast that was adapted as a bipartite tool for targeted gene expression in *drosophila*. GAL4 is a transcription factor binding to the upstream activating sequence (UAS), a genomic enhancer. Fly lines expressing GAL4 under the control of a specific promoter can be generated to drive the expression of GAL4 in various cell and tissue types. Corresponding fly lines expressing a gene of interest (gene X) downstream of the UAS sequence can then be generated. The gene X is therefore transcriptionally silent until a fly line expressing GAL4 is crossed with the flies carrying the UAS enhancer. The resulting progeny will then express gene X in a transcriptional pattern reflected by the GAL4 expression pattern which depends on the promoter driving GAL4 expression.

in the pupal stage at the end of which eclosion occurs. Females are then sexually mature 8 hours after eclosion, thus allowing the cycle to repeat itself (Hales et al., 2015) (Figure 1.4).

1.5.2 Balancers and the bipartite UAS/GAL4 system

The most attractive characteristic of flies probably is the wide range of genetic tools that have been developed over the years. For the fly's geneticist, the most precious of these tools are balancer chromosomes (Hales et al., 2015) and the UAS/GAL4 system (Brand and Perrimon, 1993).

For a genetic model such as flies, the ability to create a stable transgenic inbred stock and subsequently cross these stocks to generate an offspring with a known genotype is a prerequisite. Balancer chromosomes are the fundamental tool that enables both of these necessities. They carry a recessive lethal mutation in order to prevent the mutation of interest from being selected out other multiple crossings. Balancer chromosomes additionally carry a phenotypic marker to unambiguously identify the chromosomes inherited by each fly following a specific crossing (Greenspan, 1997; Hales et al., 2015).

The UAS/GAL4 system is a regulator of transcription in yeast that is used as a bipartite tool in transgenic drosophila to enable targeted gene expression (Brand and Perrimon, 1993). GAL4 is a transcription factor binding to the upstream activating sequence (UAS). Fly lines expressing GAL4 in a specific cell line or tissue can be generated using vectors in which GAL4 is cloned with an upstream specific promoter. A corresponding fly line expressing a gene of interest downstream of the enhancer UAS can then be generated. The transcription of the gene of interest therefore requires the concomitant expression of the GAL4 transcription factor. The absence of GAL4 in the fly line carrying the gene of interest maintains them in a transcriptionally silent state. The expression of the gene of interest is triggered by crossing the flies expressing GAL4 with the flies carrying the UAS enhancer. The resulting progeny will then express the gene of interest in a transcriptional pattern reflected by the GAL4 expression pattern which depends on the promoter driving GAL4 expression. Similarly to the fly life cycle, GAL4 activity depends on temperature. Minimal GAL4 activity is measured at 16°C while 29°C is the optimal balance between maximal GAL4 activity and minimal effects on fertility and viability (Duffy, 2002). It is therefore possible to adjust the expression level of the gene of interest or perform a conditional expression at a specific developmental stage by altering the rearing temperature (Duffy, 2002; Hales et al., 2015) (Figure 1.5).

Using these tools, fly stocks can be maintained, genotypes can be visually identified and sequences of interest can easily be expressed in specific cell types or tissues.

1.5.3 The drosophila central nervous system

The organization of the fly nervous system also makes it an attractive model. The central nervous system (CNS) of most insects including flies displays an outer layer or cortex containing cell bodies and an inner layer formed by multiple neuropiles. Neuropiles are dense regions of the brain containing numerous axons and dendrites to form circuits (Nassif et al., 2003). In insects, the brain is prolonged by a ventral nerve cord (VNC) organized in neuromeres which are parts of the CNS that process sensory inputs and control motor behavior for a single segment of the body (Niven et al., 2008). Networks in the brain and VNC are responsible for stereotyped sequences of movement called central pattern generators. In drosophila larvae, the feeding and crawling behavior are the two main stereotyped motor programs (Cardona et al., 2009). Interestingly, the crawling movement of *drosophila* larvae displayed right after hatching can still be observed when only the medial and posterior portion of the VNC is active, suggesting that the network responsible for the waves of peristaltic movements resides in this part of the nervous system. Brain inputs still seem crucial for goal directed behavior such as chemotaxis (Berni et al., 2012).

The VNC mirrors the arrangement of body segments so that motoneurons from anterior neuromeres contact muscles in the anterior part of the body whereas conversely, the most posterior muscles are innervated by motoneurons emerging from the posterior neuromeres of the VNC. In drosophila larvae, the interaction between motoneurons and muscles is known as the neuromuscular junction (NMJ) and it has been extensively studied over the years due to its simplicity, ease of study and robustness (Ruiz-Cañada and Budnik, 2006). Using presynaptic and/or postsynaptic markers, the synaptic morphology of the NMJ can be observed in a highly reproducible way by quantifying the number of synaptic boutons, their size or even fluorescence intensity (Johnson et al., 2009; Mao et al., 2014; Xiong et al., 2013).

1.5.4 Drosophila as a model for axonal transport

Drosophila models allow the study of gene mutations, overexpression and knockdown but physiological processes such as axonal transport can also be visualized with ease. Flies are thus widely used in the field of neurosciences to shed light on molecular mechanisms regulating axonal transport (Horiuchi et al., 2005) but also as models for neurodegenerative diseases (Lessing and Bonini, 2009).

Fly lines are readily accessible to express a recombinant green fluorescent protein (GFP) specifically in the mitochondria (Pilling et al., 2006) or synaptic vesicles (Zhang et al., 2002) of motoneurons. These lines can then be crossed to genetically manipulate the regulation of axonal transport and perform rescue experiments. Using these *in vivo* markers of cargoes,

axonal transport can be studied in 3rd instar larvae (Zala et al., 2013), in pupal brain explants (Medioni et al., 2015) but also in the wings of adult flies (Vagnoni and Bullock, 2016). The transparency of 3rd instar larvae and the anatomical configuration of the brain and motoneurons makes it a particularly attractive model for the study of axonal transport. The brain and the large axons of motoneurons are indeed juxtaposed to the ventral muscles of the larva transparent body, making it easy to record live-images in motoneurons using a confocal microscope.

1.5.5 Locomotor behavior assessment in drosophila

Neurodegenerative diseases are often linked with locomotor behavior defects, thus making the assessment of motor behavior primordial for the comprehensive understanding of a pathological state. The locomotor behavior of flies enables an easy and quantitative readout of motor function (Nichols et al., 2012) thus reinforcing its usefulness in the context of brain related studies.

The crawling behavior of larvae can be recorded and then analyzed to provide insights on the locomotor capacities following a pharmacological or genetic manipulation. The distance covered by the larvae as well as the number of peristaltic movements exhibited in a specific time span can be quantified. In adult flies, the climbing assay is a reproducible and easy readout of motor function. In this assay, adult flies are placed in transparent vials and mean height climbed in a specific time span is assessed. Flies with locomotor defects will tend to climb to lower heights that controls (Nichols et al., 2012).

Multiple studies have shown locomotor defects in some fly models of neurodegenerative diseases (Cragnaz et al., 2015; Lanson et al., 2011) with some highlighting motor behavior abnormalities linked with axonal transport defects (Janssens et al., 2014; Johnson et al., 2013).

1.5.6 Drosophila display a remarkable homology with mammals

Despite a smaller genome size, flies have orthologous genes for 80% of human disease-associated genes (Reiter, 2001) and all major signal transduction pathways are conserved between flies and humans (Perrimon et al., 2012). This remarkable homology between *drosophila* and mammals highlights flies as a fantastic tool for the study of gene function (Perrimon et al., 2016). In addition, the increased genome size in mammals reflects the genesis of multiple paralogs for various gene families with redundant and overlapping functions. The simpler genome of flies therefore facilitates the interpretation of loss of function studies (McGurk et al., 2015).

Relevant to my master's thesis, αTAT1, αTAT2, Elp3, ARD1, GCN5, HDAC6 and SIRT2 all have orthologs in flies based on the Uniprot database. These proteins involved in microtubule acetylation were mostly studied in mammals and *C. Elegans* therefore less is known about the

mediators of acetylation in flies. So far, only αTAT1 and HDAC6 have been linked with the regulation of microtubule acetylation in *drosophila* (Godena et al., 2014).

1.6 Aim of the master's thesis

Over the course of my master's thesis, we studied the role of dacapo -the *Drosophila Melanogaster* ortholog of p27- as a modulator of axonal transport. Based on the previous literature, we identified p27 as a candidate for the regulation of axonal transport. Some MAPs have been shown to regulate axonal transport (Vershinin et al., 2007; Basu et al., 2015) and microtubule dynamics also contribute to the modulation of transport (Moughamian et al., 2013). In this sense, the discovery that p27 is able to bind to microtubules and promote microtubule polymerization in cortical interneurons is compelling (Godin et al., 2012). Interestingly also, in mouse fibroblasts, p27 depletion resulted in a decrease of acetylated α-tubulin while p27 overexpression conversely increased α-tubulin acetylation levels (Baldassarre et al., 2005). This suggests that p27 may contribute to the regulation of acetylation levels in microtubules. As stated before, microtubule acetylation plays an important role in the speed and specificity of cargo trafficking (Reed et al., 2006; Dompierre et al., 2007; d'Ydewalle et al., 2011; Godena et al., 2014) and as such, p27 may act as a regulator of axonal transport through the modulation of acetylation levels on microtubules.

We used transgenic fly lines expressing a specific dacapo RNAi in motoneurons to knockdown dacapo. We show that the velocity of GFP-tagged mitochondria was reduced following dacapo knockdown in 3rd instar larvae mtoneurons. Using immunostainings, we then confirmed that dacapo knockdown downregulates tubulin acetylation by quantifying the acetylation levels of microtubules in dacapo depleted motoneurons. To demonstrate a causal link between decreased microtubule acetylation and axonal transport defect in dacapo depleted larvae, we rescued physiological microtubule acetylation levels using pharmacological inhibition of HDAC6 as described in previous studies (Dompierre et al., 2007). We provide data showing that the transport defect is rescued consequently to the restoration of microtubule acetylation levels, suggesting that dacapo mediates its regulatory effect on axonal transport through the modulation of microtubule acetylation. Morelli et al. (submitted) have highlighted locomotor behavior defects in dacapo knockdown larvae and adult flies that are rescued by acute HDAC6 inhibition. We therefore performed immunostainings of the larval NMJ to determine whether this defect is caused by morphological alterations to the motoneurons and their synapses. We highlighted no defect in the number of synaptic buttons of dacapo knockdown larvae, therefore suggesting that the locomotor defects do not arise from developmental alterations in NMJ morphology but rather from a malfunction of the synaptic transmission.

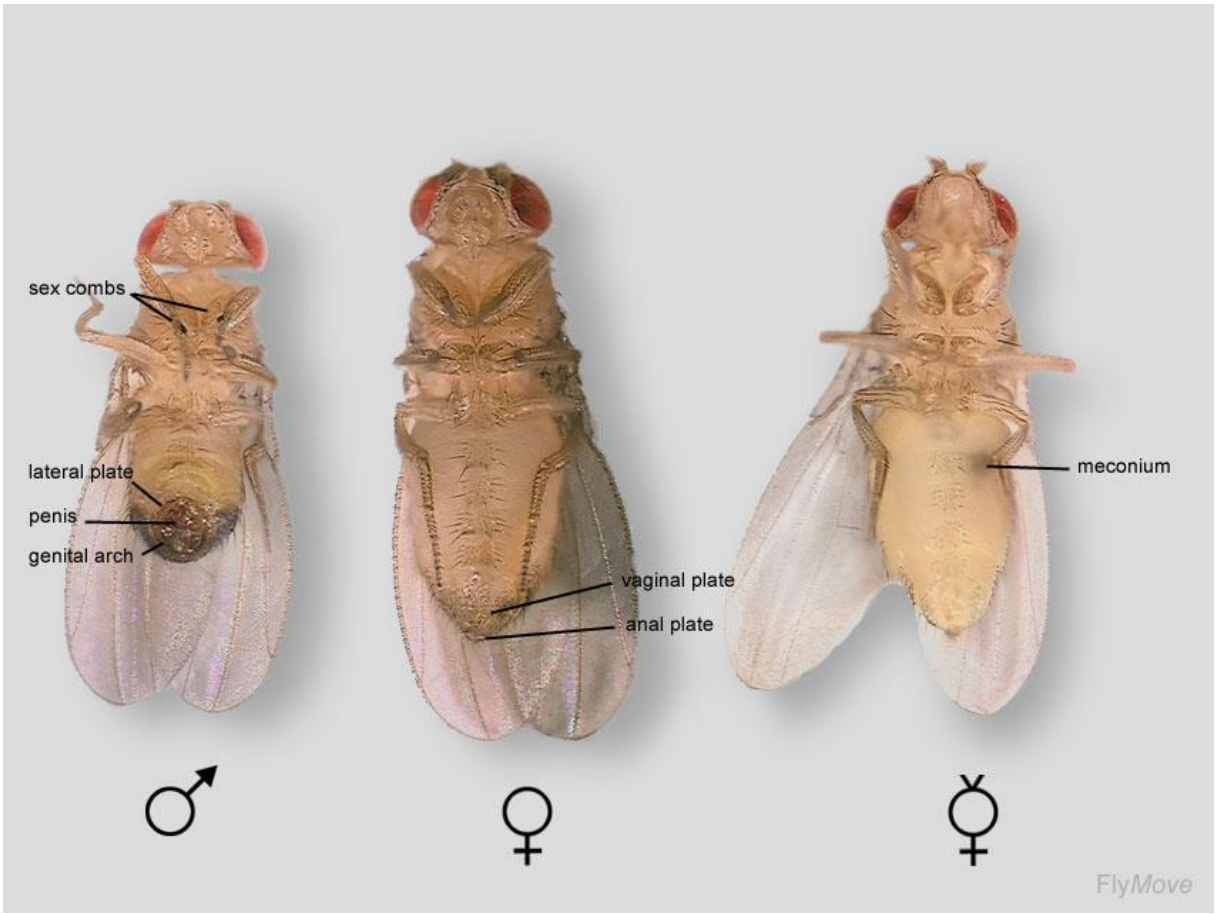

Figure 2.1: Discrimination between *Drosophila Melanogaster* males, females and female virgins (from http://flymove.uni-muenster.de)

From left to right a male (♂), female (♀) and virgin female (☿) *drosophila* under a dissection microscope. Males are on average smaller and darker than females. While females have a straight and round abdomen, the abdomen of males is thinner and slightly curved inwards. The easiest trait to distinguish males and females is the brown genitals on the postero-ventral side of males. In the 3 hours following eclosion, flies exhibit a dark spot named meconium in the upper left corner of the abdomen which corresponds to the remainings of the last meal as a larva. Since females start mating 8 hours after eclosion, the presence of the meconium is a guaranteed way to single out virgin females.

2. Material and methods

2.1 Drosophila Melanogaster work

2.1.1 Fly stocks

We used a D42-GAL4 > UAS-*mito*GFP *Drosophila Melanogaster* that expresses a specific recombinant GFP displaying a mitochondrial import sequence. The expression of GFP is driven by the D42 promoter, which is subsequently localized in the mitochondria of motoneurons and salivary glands (Pilling et al., 2006). The D42-GAL4 > UAS-*mito*GFP was crossed with specific lines expressing RNAi driven by the upstream activation sequence (UAS) (Table 2.1).

Fly line	Origin
D42-GAL4 > UAS-*mito*GFP	Bloomington Drosophila Stock Center 42737
UAS-RNAi-Dacapo	Kind gift from Pr. Perrimon
UAS-RNAi-Dacapo ; P(w+,dap1gm)III.1 (Dacapo overexpression)	Generated in the lab with P(w+,dap1gm)III.1 kindly received from Pr. Lehner (Meyer et al., 2002)
UAS-RNAi-ZPG	Vienna Drosophila Resource Center CG10125

Table 2.1: Sources of the fly lines used in this thesis

2.1.2 Culture conditions and husbandry

Flies were reared in a standard culture medium adapted from Bloomington Drosophila Stock Center recipes (http://flystocks.bio.indiana.edu). The medium was prepared by mixing in hot water for approximately one hour: brewer yeast extract (Acros Organics 368080050), corn flour (Genesee Scientific #62100), agar (Sobigel SB12073) and the antimycotic methyl 4-hydroxybenzoate (Acros Organics 126965000) at a concentration of 2.5g/L. Once dense, the medium was poured into plastic vials and dried overnight. Foam caps were then used to close the vials which were kept at 4°C for optimal conservation or 20°C for experimental purposes.
The fly lines were maintained at 25°C and 20°C; the former temperature was utilized to promote the production of D42-GAL4 > UAS-*mito*GFP virgin females for crossing whereas the latter was employed for rigorous control of fly life-cycle and husbandry.

2.1.3 Crossings

Males and females were segregated based on their morphological differences as described in Figure 2.1. Males are on average smaller than females and their abdomen is thin and slightly curved inwards. Conversely the abdomen of females is straight and round (Greenspan, 1997).

The genital apparatus of males appear as a relatively large brown mass in the postero-ventral part of the abdomen while the female genitals are less noticeable (Greenspan, 1997). Virgin females were singled-out based on the presence of the meconium, a dark spot in the upper left corner of the abdomen which is visible up to 3 hours after eclosion (Greenspan, 1997). Since females do not mate in the first 8 hours following eclosion, the presence of the meconium guarantees the virginity of the females (Greenspan, 1997).

Balancer chromosomes carry a dominant marker mutation and are recessive lethal. Based on these properties, flies can only carry one or no balancer chromosome and they can be discriminated based on the dominant phenotypic marker expressed on the balancer chromosome (Hales et al., 2015b). Cyo flies carrying the balancer will exhibit curled wings (*Cy* marker) while TM6B flies, larvae and pupae are shorter and thicker than wild-types (*Tubby* marker). To obtain a homogenous heterozygote progeny from a crossing, it is required to cross homozygous virgin females with homozygous males. Flies carrying a balancer chromosome must therefore be excluded based on the phenotypic trait they display. Some of the fly lines used in Table 2.1 carried balancer chromosomes. To ensure the homogeneity of the progeny, only homozygous males carrying neither *Cy* or *Tubby* were crossed with D42-GAL4 > UAS-*mito*GFP virgin females. Females and males were kept for a duration of 2 to 3 days at 25°C and then transferred in a new vial. The eggs laid over the course of this period were kept at 29°. This temperature has been determined as the optimal balance between maximal GAL4 activity and minimum effects on fertility and viability (Duffy 2002). 3rd instar larvae were collected 5 to 6 days after the start of the crossing and were used for immunohistochemistry or transport studies. Due to inter-individual variability, each larva was checked on an epifluorescent microscope before experiments to ensure that GFP was expressed.

2.2 Drug administration

When tubastatin treatment was required, tubastatin A 1mM (Sigma) or an equivalent amount of dimethyl sulfoxide (DMSO) were diluted in a 10% sucrose solution. Larvae were then incubated in the solution for 30min using a 24 well plate with 500µL per well. After incubation, larvae were dried properly and dissected immediately for immunohistochemistry or anesthetized for time-lapse imaging of transport.

2.3 Larval dissection for immunostainings of motoneurons or neuromuscular junction

This protocol is adapted from (Brent et al. 2009) and (Devireddy et al. 2014).

Materials:

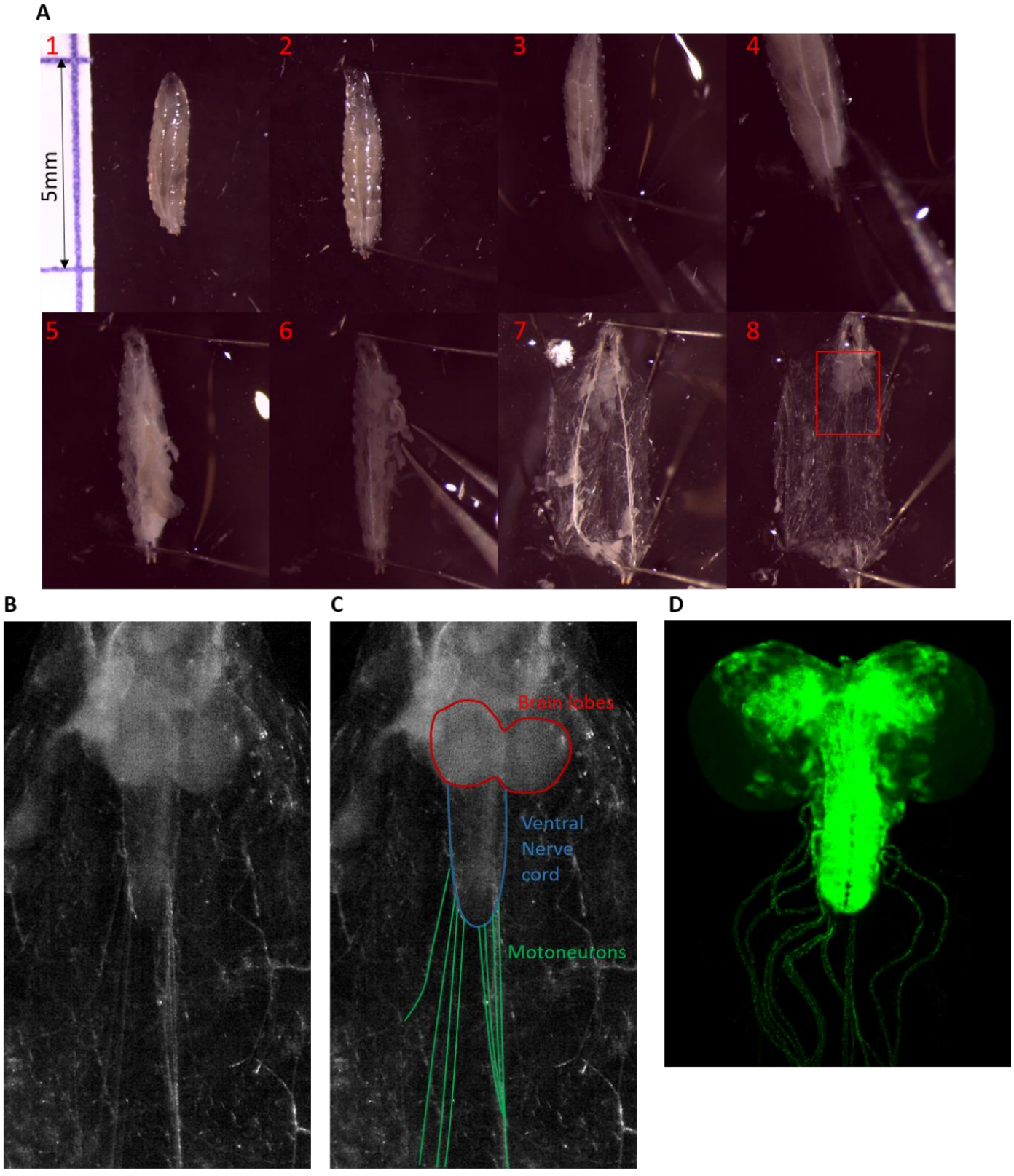

Figure 2.2: Critical steps of larval dissection and CNS representation
(A) Critical steps of the larva dissection, in all frames the anterior part is up. In order, the larva is placed on the dissection plate **(1)**, it is then pinned at its anterior and posterior extremity **(2)**. PBS is added and a hole is pierced adjacent to the posterior pin **(3)** and a longitudinal cut from the posterior to the anterior end is performed **(4)**. The organs are floating in PBS **(5),** making it easier to remove those using fine forceps **(6).** When most organs have been removed, 4 pins are inserted to flatten the body walls **(7)** and the remaining organs are removed **(8). (B)** Magnification of the frame drawn in **(A8)**. **(C)** Annotated version of **(B)** highlighting the brain lobes, ventral nerve cord and motoneurons. **(D)** Confocal image of a 3rd instar larva D42 > *mito*GFP brain at 20x after dissection.

Dissection microscope (Leica M80) with incident illumination
Vannas iris scissors (Aesculap OC498R)
Two pairs of forceps (Fine Science Tools - Dumostar #55)
Minutien insect pins (Fine Science Tools #26002-10)
Homemade Sylgard plate with small edges (Sylgard 184 Silicone Elastomer Kit from Dow Corning)
PBS buffer
PFA 4%
10% sucrose solubilized in distilled water.

1mL of the sucrose solution at room temperature was added in each well of a 12-wells plate and 3rd instar larvae were segregated in the wells according to their genotype. The sucrose solution ensures that larvae have access to food while preventing them from crawling on the walls of the petri dish. Larvae were usually kept for a maximum of one hour in this solution before a new batch was collected. Once in the sucrose solution, the GFP expression is checked with a binocular epifluorescent microscope. The larvae exhibiting no GFP in the nervous system and salivary glands were excluded.

The description of the procedure is illustrated with 8 key frames in Figure 2.2A which are referred to only by their number in the following text. A larva was transferred from a well to the Sylgard plate with the ventral part of the body facing downwards to make the pharyngeal tubes apparent **(1).** An insect pin was then inserted through the posterior part of the body between the pharynges. A second pin was inserted in the anterior part between the mouth hooks to slightly stretch the larva and hold it in place **(2)**. 100µL of PBS was added to submerge the larva in order to make internal organs float which facilitated their removal **(5)**. Using a larger pin, a small hole was created by gently pulling on the skin that was pierced at the posterior end **(3)**. A longitudinal cut along the midline was then performed starting from the posterior end to the anterior end **(4)**. This step is critical as the integrity of the nervous system must be preserved. To avoid damaging motoneurons or the brain, the cut must be made just underneath the larval body wall. Organs (fat, salivary glands, intestine, pharyngeal tubes) were grossly removed with fine forceps **(6)** while avoiding strong pulling forces on the segmental nerves. 4 pins were then placed on the 4 extremities of the body wall to flatten the larva and stretch it in a horizontal and vertical manner **(7).** The remaining organs were then carefully removed to leave only the CNS and peripheral nerves **(8)**. Higher magnifications of the brain revealed by the dissection are shown in Figure 2.2 B-D. The PBS was removed using a micropipette and 100µL of PFA 4% was added. After 20 minutes at room temperature, the PFA was removed and the larva was

washed 3 times with PBS. The pins were then gently pulled while holding the body of the larva to prevent ripping. The dissected larvae can either be used for immunostaining directly or they can be stored at 4°C for a few weeks in a plastic container filled with PBS.

2.4 Immunohistochemistry and confocal imaging of dissected larvae

Immunochemistry experiments were performed in glass dishes with a spherical bottom which makes it easy to remove and add liquid without damaging the larvae. The antibodies used were tubulin 1:150 from sheep (Cytoskeleton ATNO2), acetylated-tubulin 1:5000 from mouse (Sigma, T6793), horse raddish peroxidase (HRP) 1:1000 from rabbit (Sigma) and cysteine string protein (CSP) 1:10 from mouse, kindly gifted by S. Benzer. Secondary antibodies against the appropriate species were used with a 1:500 dilution.

Larvae were washed 3 times in PBS 0.3% Triton X-100 for 5 minutes and incubated for 30 minutes in the blocking solution of PBS 0.3% Triton X-100 and 1% bovine serum albumin (BSA). Larvae were incubated at 4° over-night in the primary antibodies diluted in the blocking solution. To prevent evaporation of the solution, the dish was covered with parafilm. Larvae were then washed 3 times in PBS 0.3% Triton X-100 for 5 minutes and incubated for 2 hours at room temperature in the secondary antibodies diluted in the blocking solution. Larvae were washed 3 times in PBS 0.3% Triton X-100 for 5 minutes and immediately mounted on glass slides with the nervous system facing upwards. A maximum of 3 larvae were mounted per slide using 100µL of the mounting medium Mowiol. The slides were kept at room temperature for a few hours for the Mowiol to dry and then stored at 4°C until imaging.

This protocol was used for tubulin/acetylated tubulin stainings. The protocol for CSP/HRP staining is identical but PBS 0.2% Triton X-100 was used at each step.

Larvae were imaged using a Nikon A1Ti inverted confocal microscope. For quantitative analysis, laser power, gain and offset were optimized to avoid surexposition while maintaining adequate sensitivity. The optimized settings were used throughout experiments to ensure samples were comparable. Imaging of tubulin/acetylated tubulin stainings was performed using the 60x oil-immersed objective while the 40x oil-immersed was used for CSP/HRP.

2.5 Preparation of the larvae for transport live-imaging

Larvae were collected in sucrose 10% and the GFP expression was checked as described before. A maximum of 3 larvae were then dried on absorbing paper and placed in a perforated falcon cap. The closed falcon was placed upside down in a sealed beaker containing paper soaked in ether. Larvae were kept in the ether fumes for 8 minutes, a duration optimized by Morelli et al. to ensure survival and efficient anesthesia. Each larva was then placed on a glass slide with the

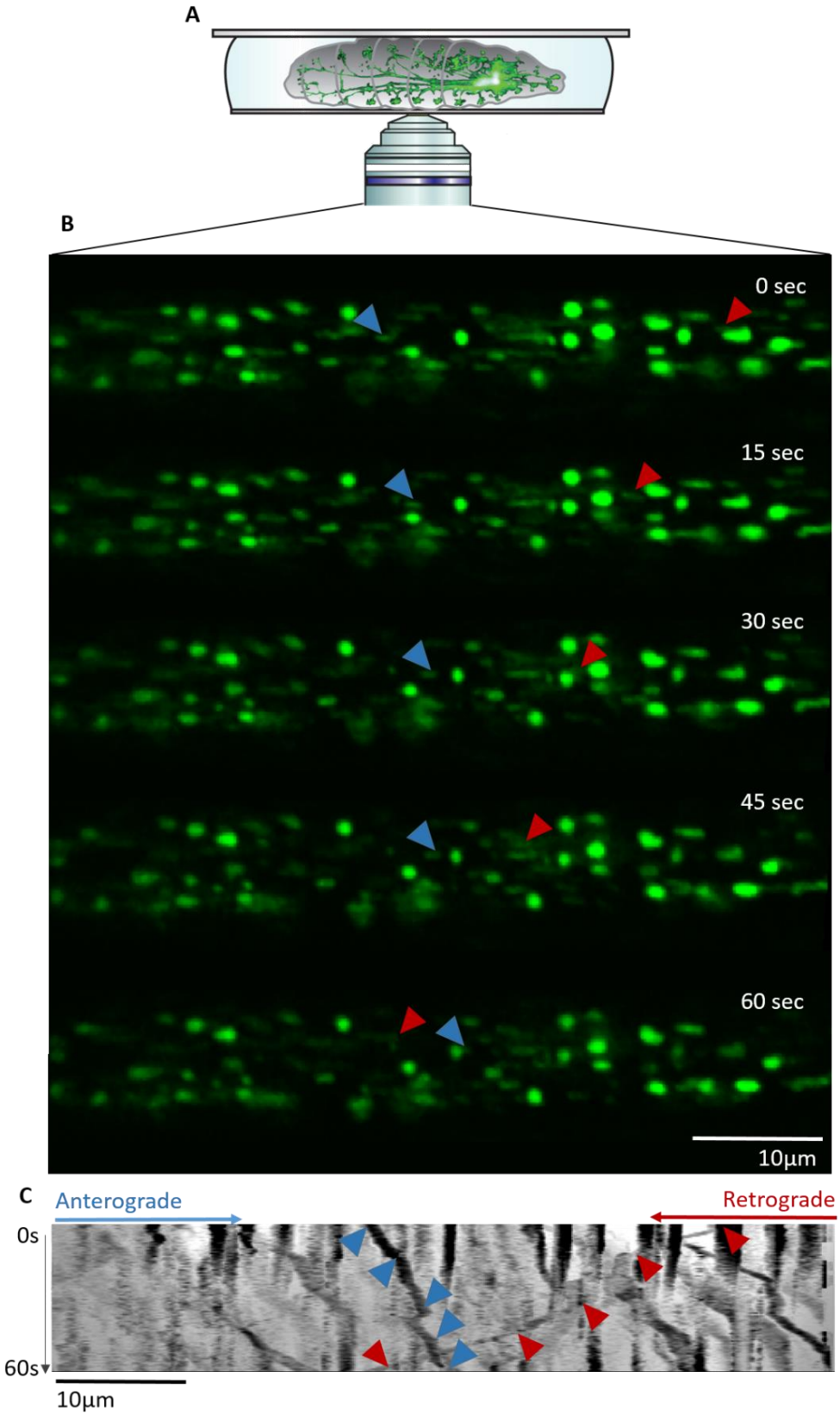

Figure 2.3: Live-imaging setup and illustration of mitochondria transport
(A) The anesthetized larva is mounted on a glass slide with a drop of 80% glycerol and a coverslip. The brain and motoneurons can be seen through the transparent body wall using an inverted confocal microscope (from Morelli et al., in revision) **(B)** Five frames of a 1 minute movie recording GFP-tagged mitochondria in a motoneuron. Blue and red arrows track a single mitochondrion moving respectively in the anterograde and retrograde direction. (C) Kymograph generated by KymoToolBox. Time is shown on the y-axis and distance on the x-axis. The trajectories of the mitochondria marked with the arrows in (B) can be seen on the kymograph.

ventral side facing upwards. A drop of glycerol 80% was added and the larvae were flattened gently using a coverslip stuck with nail-polish (Figure 2.3A). The transport of mitochondria was then imaged using a Nikon A1Ti microscope in resonant mode at 600ms interval during 1 minute with the 60x oil-immersed objective. An example of the captured images is shown in Figure 2.3B. Larvae display slight variations in the intensity of GFP expression and therefore laser power, gain and offset were adjusted between animals to maximize the visibility of mitochondria. Three movies were recorded for each larva, ensuring that the time elapsed between anesthetization and imaging never exceeded 30 minutes.

2.6 Analysis and statistics

For tubulin/acetylated tubulin stainings, the fluorescence intensity of 10 motoneurons was quantified per larva using ImageJ. The ratio between tubulin and acetylated tubulin was then calculated and normalized to control.

For CSP/HRP stainings, two NMJs were imaged for segments 3 to 5, for a total of 6 NMJs per larva. Multiple images were taken in the Z plan to ensure that all buttons were imaged. A maximum intensity projection was then performed and the number of synaptic boutons per NMJ was counted using the ImageJ cell counter.

For time-lapse movies of mitochondria transport, slight movements of the larvae were first compensated using the StackReg ImageJ plugin. Kymographs were then generated and analyzed using the KymoToolBox plugin as shown in Pineda et al. 2009. The kymographs generated by this plugin report the position of mitochondria along the x axis and the time elapsed along the y axis (Figure 2.3C). The mitochondria trajectories can then be manually drawn to extract the speed and direction of their movement. Mitochondria with speeds inferior to 0.1µm/sec were considered as stationary and were thus excluded from the analysis.

Statistical analysis was performed using the GraphPad Prism 7.0 software. D'Agostino & Pearson, Shapiro-Wild and KS normality tests were performed for each analysis. If the data displayed a normal distribution, an unpaired t-test or one-way ANOVA with Bonferroni post-hoc test were performed. Conversely, if the distribution was not normal, a Kruskal-Wallis with Dunn's post-hoc test were performed. The criterion for statistical significance was set at $p < 0.05$ with * = p<0,05, ** = p<0,01, *** = p<0,001, ****=p<0,0001.

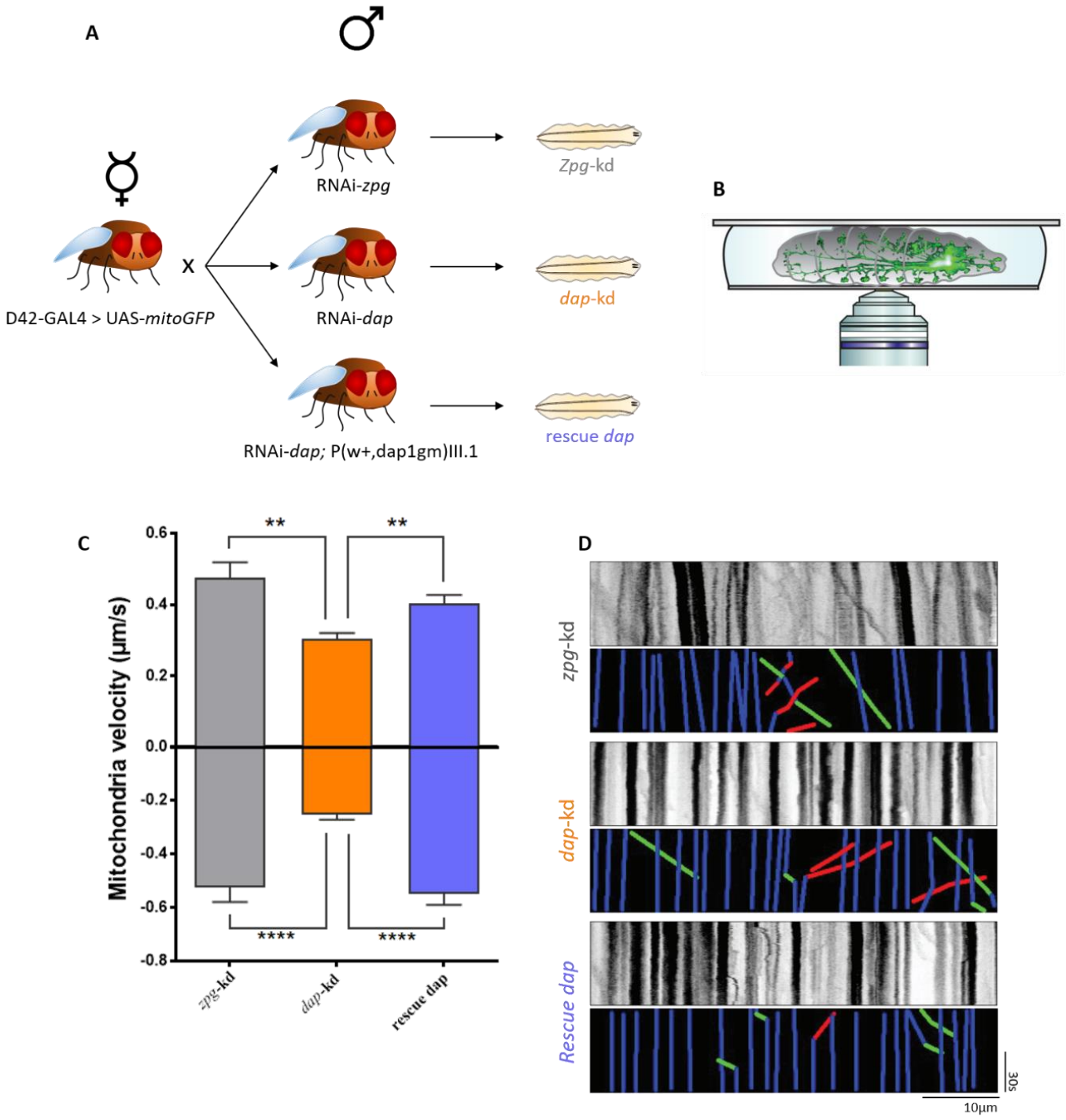

Figure 3.1: *dacapo* knockdown slows down mitochondria transport *in vivo*
(A) D42-GAL4 > UAS-*mitoGFP* virgin females were crossed with RNAi-*zpg*, RNAi-*dap* and RNAi-*dap*; P(w+,dap1gm)III.1 males to respectively generate *zpg*-kd, *dap*-kd and rescue *dap* larvae. **(B)** 3rd instar larvae from these crossings were then anesthetized and mounted on glass slides for live-imaging of the GFP positive mitochondria. **(C)** Quantification of mitochondria velocity based on live-imaging of *zpg*-kd, *dap*-kd and rescue *dap* larvae. Positive and negative values represent anterograde and retrograde movement respectively. Values are mean ± standard error of the mean and were analyzed using the non-parametric Kruskal-Wallis test followed by Dunn post hoc-tests. ** p<0,01, ***p<0,001, **** p<0.0001. N (of mitochondria) is > 50 with at least 5 animals per condition. **(D)** Representative kymographs and their corresponding colored kymographs. Green, red and blue lines represent respectively anterograde, retrograde and stationary mitochondria.

3. Results

3.1 Dacapo knockdown slows down mitochondria and vesicular transport

p27, the mammalian ortholog of dacapo, has previously been shown to interact with microtubules and promote their polymerization (Godin et al., 2012) while in mouse fibroblasts, p27 depletion resulted in a decrease of acetylated α-tubulin (Baldassarre et al., 2005). Since a correlation between microtubule acetylation and the regulation of transport has been established in several studies (Dompierre et al., 2007; Godena et al., 2014; Reed et al., 2006), we tested whether the p27 fly ortholog dacapo is involved in the regulation of axonal transport.

D42-GAL4 > UAS-*mito*GFP flies express a recombinant GFP displaying a mitochondrial import sequence thus enabling the transport of newly synthesized GFP to mitochondria (Rizzuto et al., 1995). The D42 promoter drives efficient expression of GAL4 specifically in motoneurons (Sanyal, 2009). We crossed D42-GAL4 > UAS-*mito*GFP female virgins with the three lines listed in Table 1 to assess the consequences of *dacapo* knockdown on transport (Figure 3.1A). The efficiency of dacapo knockdown in *dap*-kd larvae as well as the rescue of its expression level in rescue *dap* has been shown by Morelli et al. (submitted). Zero Population Growth (*zpg*) is a gene only expressed in the germline of flies (Tazuke et al., 2002). The expression of a RNAi targeted towards *zpg* mRNA is therefore used as a control for brain related studies involving knock-down experiments (Zala et al., 2013).

Lines crossed with D42-GAL4 > *mito*GFP	**Designation of the progeny**
UAS-RNAi-zpg	*zpg*-kd
UAS-RNAi-*dacapo*	*dacapo*-kd
UAS-RNAi-*dacapo*; P(w+,dap1gm)III.1	rescue *dap*

Table 1: Crossings performed and their corresponding nomenclature.

We performed time-lapse imaging of mitochondria transport in anesthetized *zpg*-kd, *dap*-kd and rescue *dap* 3rd instar larvae. Time-lapse recordings of the moving GFP-expressing mitochondria in motoneurons were recorded through the body walls using a confocal microscope (Figure 3.1B). Both retrograde and anterograde transport of mitochondria had a markedly reduced velocity following *dap* knockdown (Figure 3.1C-3.1D) while genetic re-expression of *dap* restored retrograde and anterograde transport velocities. Additionally, data collected by Morelli et al. (unpublished) shows that synaptic vesicles marked with synaptotagmin-GFP display the same defects in anterograde and retrograde velocities (Supplementary Figure 3.1A-3.1B). Taken together, these results reveal that dacapo is implicated in the modulation of axonal transport for both mitochondria and synaptic vesicles in 3rd instar larvae.

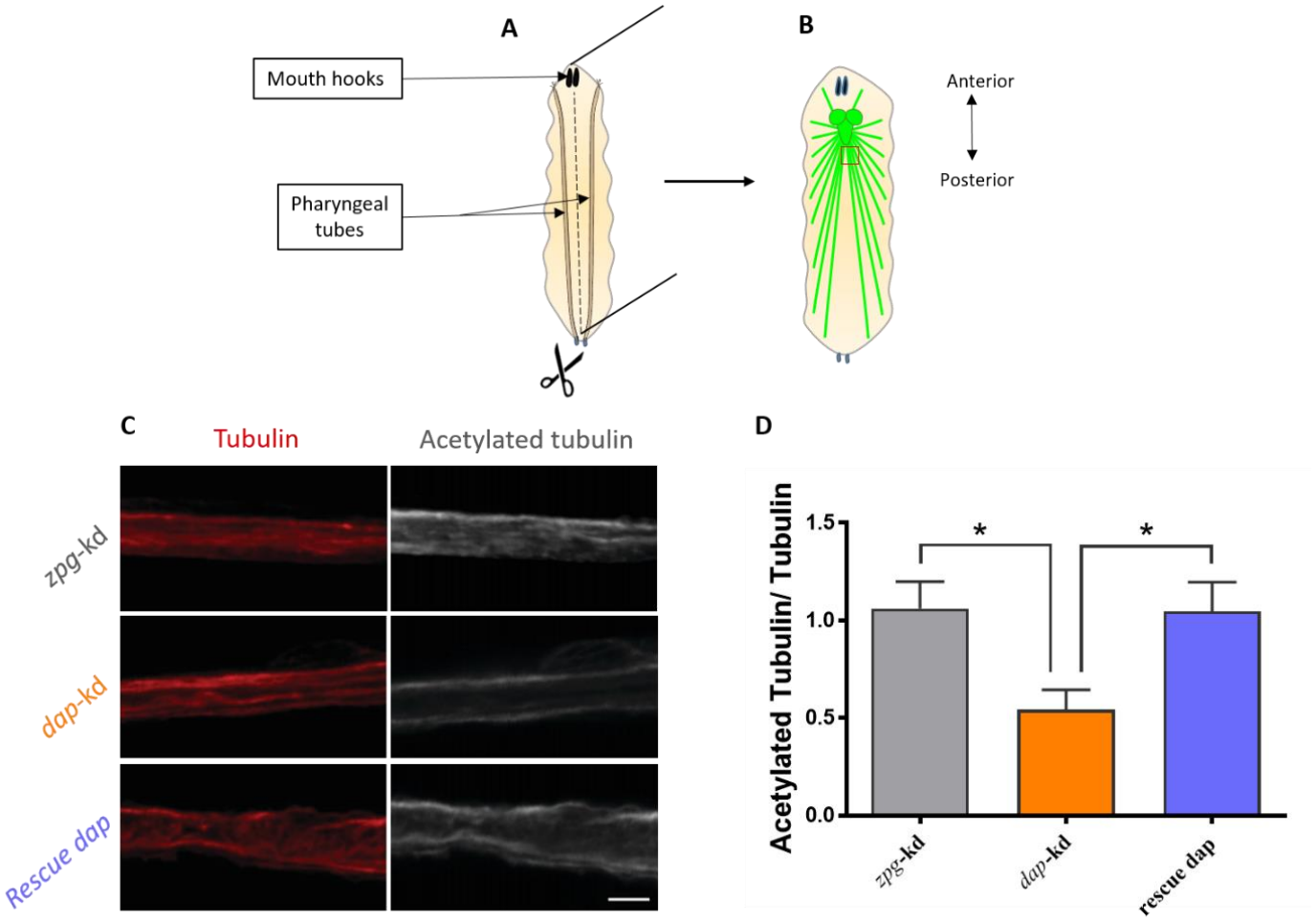

Figure 3.2: *dacapo* knockdown results in reduced microtubule acetylation in motoneurons
(A) Schematic drawing of a larva depicted with its mouth hooks and pharyngeal tubes. A midline-sagittal incision starting from the posterior end in a caudal to rostral direction is performed as represented by the dotted line. **(B)** Exposed GFP-expressing brain and motoneurons after the larva body walls are flattened. Images were taken in the area marked by the red square. **(C)** Representative images of the proximal motoneurons immunostained for tubulin (red) and acetylated tubulin (white) in *zpg*-kd, *dap*-kd and rescue *dap*. Scale bars represents 10µm **(D)** Quantification of acetylated tubulin on tubulin fluorescence intensity ratio normalized to *zpg*-kd controls. One-way ANOVA followed by Bonferroni post-hoc test was performed, **** p<0,0001 Values represent mean ± SEM with n=9 (*zpg*-kd), 8 (*dap*-kd), 8 (rescue *dap*).

3.2 Optimization of *drosophila* larvae dissection

We optimized a dissection protocol to assess microtubule acetylation levels in larvae. The immunostaining of axons for tubulin and acetylated tubulin enables a readout of the fluorescence intensity in a robust and reproducible way, as shown in previous studies using this technique (Bhagwat et al., 2014; Szyk et al., 2014). We thus optimized the larval sample preparation to perform co-staining of tubulin and acetylated tubulin in larval motoneurons.

3.2.1 Larval CNS isolation

We first followed Wu and Luo, 2006 protocol for larval CNS isolation in order to stain motoneurons. The brain was dissected by pulling on the mouth hooks while holding the mid body of the larva. Although this dissection method is fast, the preservation of the tissue while carrying out the immunochemistry was hindered due to the exposition and vulnerability of the brain. The motoneurons were also severed as the CNS was separated from the rest of the body. As a result, the motoneurons left on the brain were short and tended to curl and overlap which was not optimal for the quantification of immunofluorescence intensity.

3.2.2 Larval body dissection

We overcame these technical problems by optimizing another published larva dissection technique (Brent et al., 2009; Devireddy et al., 2014). The steps we followed in the optimized protocol are detailed in the material and methods section. To setup this technique, we first had to manufacture a transparent silicon elastomer dissection plate using Sylgard. Since the larva dissection requires the use of tools in a horizontal position, specifically when the skin is cut, the plate had to have low edges. We used standard fine forceps to hold the larvae and remove the internal organs as well as ophthalmic scissors to cut the body walls of the larvae. Insect pins with a sharp tip and very fine diameter were used to restrain the larvae and stretch out the body walls after the cut was made. A larger pin was used to pierce a hole at the posterior part of the body in which we inserted the scissors.

The integrity of the body walls was not a prerequisite for the immunostaining of acetylated microtubules. Therefore we adapted the protocol of Brent *et al.* by using only two pins in the anterior part of the body in order to stretch out the body walls and expose the brain and motoneurons (Fig. 3.1A-3.1B). In this experiment, the rest of the body was used to hold the larva and protect the CNS while carrying out the immunochemistry. Using this dissection method, the full body of the larva was preserved and motoneurons remained connected to the muscles. Altogether this dissection protocol is more time consuming than the one described in Wu and Luo, 2006 but motoneurons are better preserved which subsequently allows us to

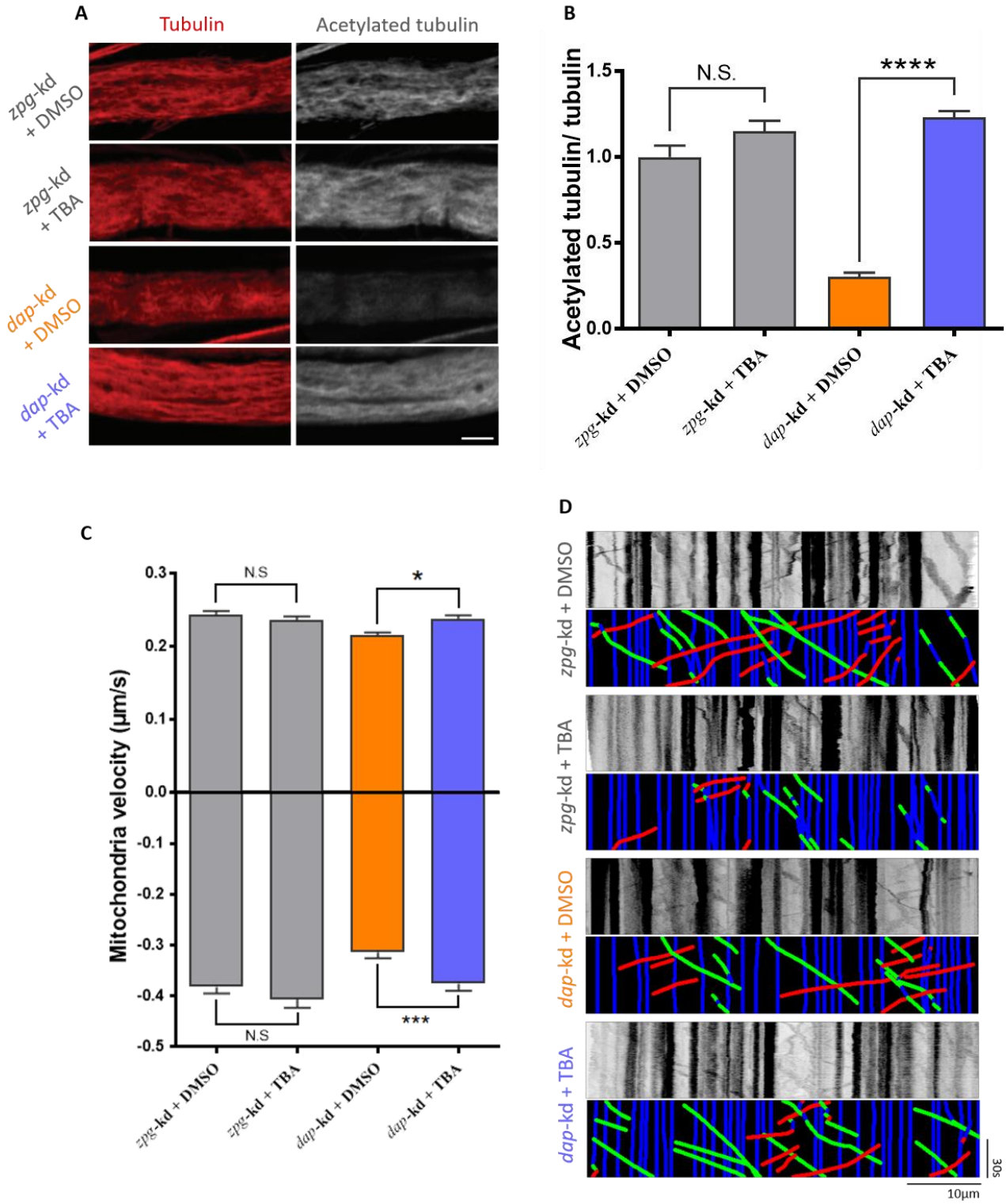

Figure 3.3: Tubastatin treatment rescues microtubule acetylation and mitochondria velocity in *dap*-kd
(A) Representative images of motoneurons immunostained for tubulin (red) and acetylated tubulin (white) from *zpg*-kd and *dap*-kd larvae fed for 30min with 1mM DMSO or tubastatin A (TBA) sucrose solution. Scale bars are 10µm **(B)** Quantification of acetylated tubulin on tubulin fluorescence intensity ratio normalized to *zpg*-kd controls. One-way ANOVA followed by Bonferroni post-hoc test was performed. Values represent mean ± SEM with n=7 (*zpg*-kd + DMSO), 11 (*zpg*-kd + TBA), 9 (*dap*-kd + DMSO), 10 (*dap*-kd + TBA). **(C)** Quantification of mitochondria velocity based on live-imaging of *zpg*-kd and *dap*-kd larvae fed for 30min with either 1mM DMSO or tubastatin A (TBA) sucrose solution. Positive and negative values represent anterograde and retrograde movement respectively. Values are mean ± standard error of the mean and were analyzed using the non-parametric Kruskal-Wallis test followed by Dunn post hoc-tests. N of mitochondria > 150 with N of animals = 6 per condition. **(B-C)** N.S. = non-significant, * p<0.05, ***p<0,001, **** p<0.0001 (**D**) Representative kymographs and their corresponding colored kymographs. Green, red and blue lines represent respectively anterograde, retrograde and stationary mitochondria.

analyze up to ten straight motoneurons for each larva. This in turn ensures a more robust quantification of fluorescence intensity.

For the immunostainings of the NMJ, we adapted a published protocol (Brent *et al.*, 2009 and Devireddy *et al.*, 2014). We first tried to make four small lateral cuts at the left and right side very close to the anterior and posterior part of the body as described in the protocol. However this manipulation was unnecessarily traumatic for the body walls as the longitudinal cut from the posterior part to the anterior part of the body was sufficient to flatten the body walls. By putting the insect pin very close to the posterior end of the larva, we could then cut from the posterior pin to the anterior one and slightly stretch out the body walls using four pins at the extremities. This dissection technique allowed us to visualize the NMJ while maintaining the attachment of the segmental nerves to the body walls.

3.3 *dacapo* knockdown results in markedly reduced tubulin acetylation

Since microtubule acetylation is linked to the regulation of transport (Dompierre et al., 2007; Godena et al., 2014; Reed et al., 2006) and p27 depletion results in a decrease of acetylated α-tubulin (Baldassarre et al., 2005), we tested whether *dap*-kd larvae exhibit decreased tubulin acetylation. The larval body wall was cut longitudinally from the posterior to the anterior end in order to expose the GFP expressing brain and motoneurons in *zpg*-kd, *dap*-kd and rescue *dap* 3rd instar larvae (Figure 3.2A-3.2B). We then performed a co-immunolabeling of tubulin and acetylated tubulin and measured the fluorescence intensity of both markers in motoneurons to calculate the ratio of acetylated tubulin on tubulin normalized to *zpg*-kd controls (Figure 3.2C-3.2D).

We observed a marked reduction of acetylation levels in *dap*-kd larvae, which was rescued upon genetic re-expression of *dap*. The decrease of microtubule acetylation displayed in *dap*-kd larvae is likely caused by a specific dacapo knockdown since the rescue of *dacapo* expression restores basal levels of acetylation. Together these results suggest that dacapo is required to maintain physiological levels of α-tubulin acetylation in 3rd instar larvae motoneurons.

3.4 HDAC6 inhibition in *dacapo* knockdown rescues microtubule acetylation and axonal transport velocity

3.4.1 HDAC6 inhibition by tubastatin restores microtubule acetylation levels in dap-kd

Pharmacological or genetic inhibition of the tubulin deacetylase HDAC6 have been shown to rescue axonal transport defects by increasing microtubule acetylation (d'Ydewalle et al., 2011; Dompierre et al., 2007; Godena et al., 2014). We therefore carried out rescue experiments to

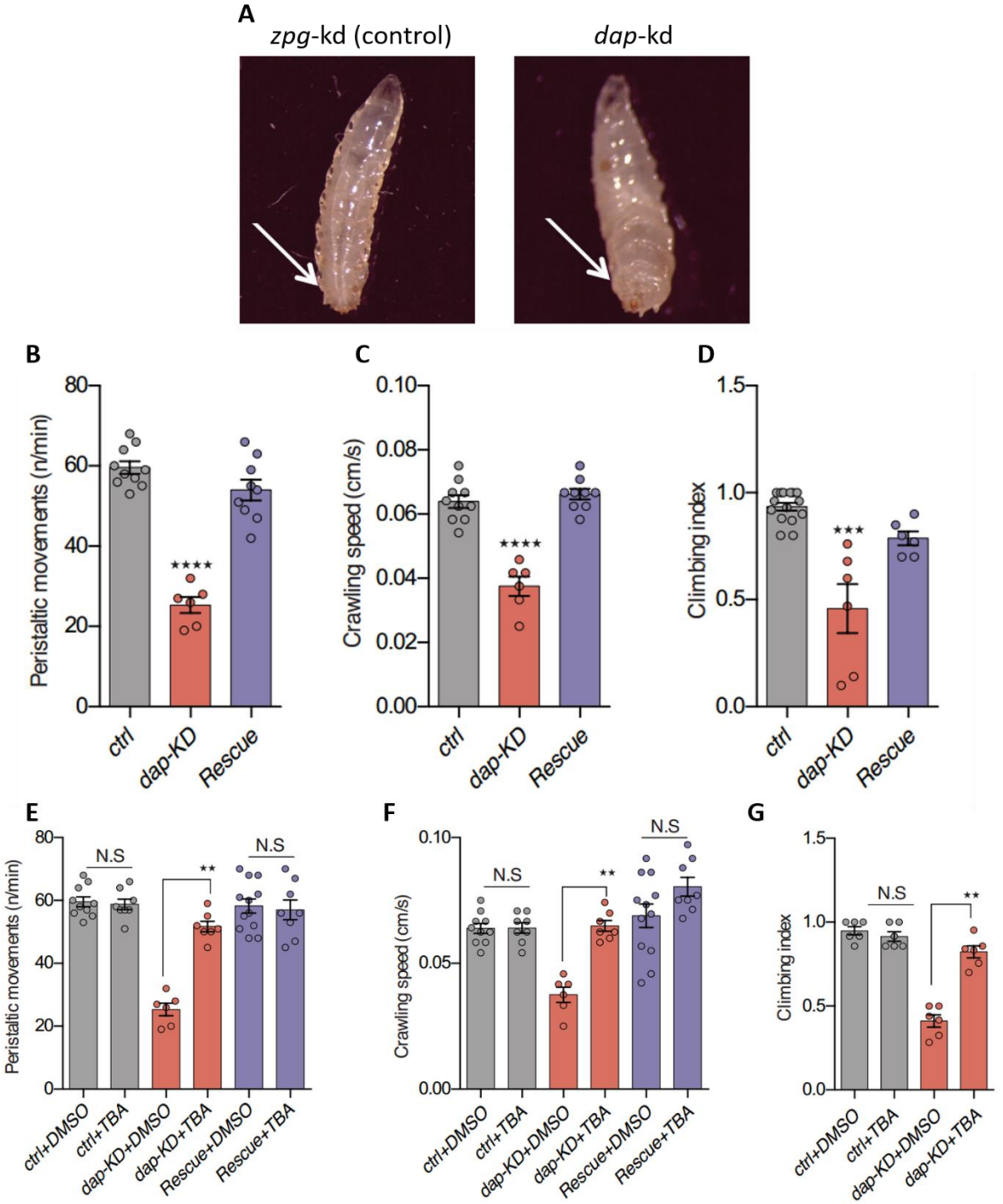

Figure 3.4: *dacapo* knockdown induces locomotor defects that are improved with tubastatin treatment
Results from Morelli et al. (submitted). (A) Representative picture of the "tail flipping phenotype" in *zpg*-kd (control) vs *dap*-kd 3rd instar larvae. *dap*-kd larvae exhibit an upward motion of the posterior end not displayed by control larvae. Number of peristaltic movements (B-E), crawling speed (C-F) were measured in 3rd instar larvae and climbing index in adult flies (D-G). (E-F-G) Larvae and adult flies were fed with 1mM DMSO or tubastatin (TBA) soaked food prior testing. (B-C-E-F) 3rd instar locomotion was analyzed using one-way ANOVA followed by Bonferonni post-hoc test with n=10 (ctrl), 6 (*dap*-kd), 9 (rescue), 10 (ctrl + DMSO), 8 (ctrl + TBA), 10 (*dap*-kd + DMSO), 7 (*dap*-kd + TBA). (D-G) Adult flies behavior was analyzed using Kruskal-Wallis followed by Dunn post-hoc tests with n=13 (ctrl), 6 (*dap*-kd), 6 (Rescue), 6 (ctrl + DMSO), 6 (ctrl + TBA), 6 (*dap*-kd+ DMSO), 6 (*dap*-kd + TBA). N.S. = non-significant, **p<0.01, ***p<0,001, **** p<0.0001.

consolidate the link between the level of α-tubulin acetylation and the velocity of axonal transport in *dap*-kd. To this aim, we used tubastatin, a specific HDAC6 inhibitor (Butler et al., 2010) that promotes increase of acetylation of microtubules (Godena et al., 2014). We first assessed whether the reduction of microtubule acetylation observed in *dap*-kd animals could be rescued by tubastatin. *zpg*-kd and *dap*-kd larvae were incubated for 30 minutes in 1mM of tubastatin or an equivalent concentration of DMSO. Optimization of tubastatin concentration and time of exposure have been determined by Morelli et al. (submitted). Following tubastatin treatment, larvae were washed with PBS and dissected in order to perform the immunohistochemistry for acetylated tubulin and tubulin. *zpg*-kd larvae treated with tubastatin exhibited a non-significant increase in the ratio of acetylated tubulin on tubulin compared to DMSO treatment (Figure 3.3A-3.3B). On the other hand, tubastatin treatment in *dap*-kd larvae dramatically increased the levels of acetylation compared to DMSO. The ratio of acetylated tubulin on tubulin was indeed comparable between *zpg*-kd treated with tubastatin and *dap*-kd treated with tubastatin. These observations show that HDAC6 inhibition with tubastatin restores the level of microtubule acetylation in *dap* knockdown to basal condition.

3.4.2 Transport velocity is rescued with tubastatin treatment

As shown before, tubastatin treatment for 30min at 1mM is able to restore a ratio of acetylated tubulin on tubulin comparable to controls. We thus treated *zpg*-kd and *dap*-kd larvae with tubastatin or DMSO and measured the velocity of mitochondria transport (Figure 3.3C-3.3D). *zpg*-kd larvae treated with DMSO or tubastatin exhibited no significant difference in the velocity of mitochondria. As expected, mitochondria from DMSO treated *dap*-kd larvae exhibited lower velocities than the mitochondria of DMSO treated *zpg*-kd for both anterograde and retrograde transport. However tubastatin treatment in *dap*-kd remarkably restored the anterograde and retrograde velocity of mitochondria to levels similar to controls. The rescue in transport is also displayed with synaptotagmin-GFP synaptic vesicles, as shown by Morelli et al. (submitted) (Supplementary Figure 3.1C-3.1D). Taken together, these results show that HDAC6 pharmacological inhibition raises the levels of microtubule acetylation in *dap*-kd and subsequently rescues the velocity of mitochondrial and vesicular transport, which suggests a causative link between microtubule acetylation and the modulation of axonal transport.

3.5 *dacapo* knockdown results in locomotor defects without alterations of the NMJ

Several studies have linked axonal transport defects with motor behavior defects in *drosophila* larvae (Janssens et al., 2014; Johnson et al., 2013). *dap*-kd larvae display a “tail flipping” phenotype characterized by an upward motion of the posterior segments during crawling

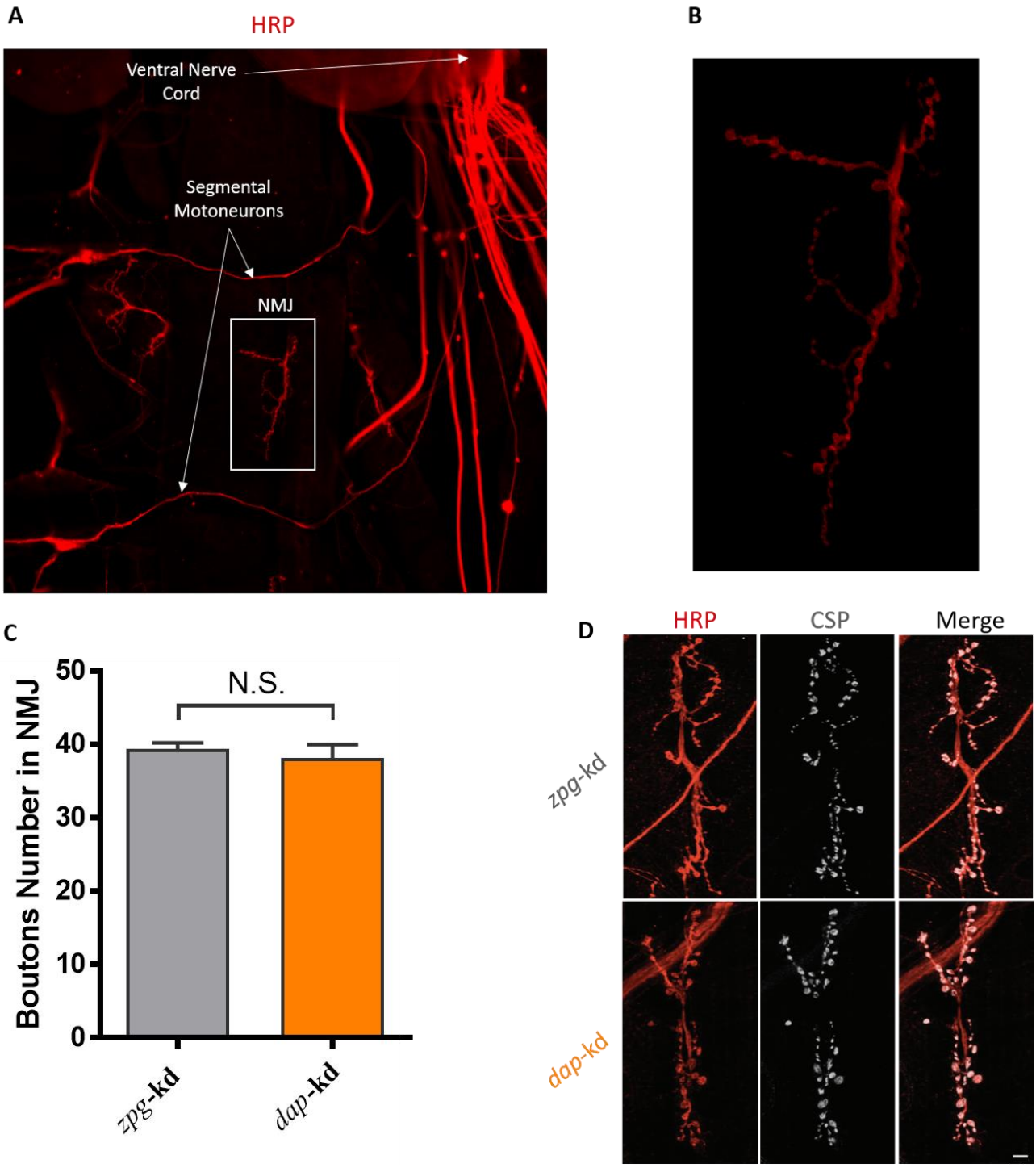

Figure 3.5: NMJ morphology is unaffected by *dacapo* knockdown
(A) 20x picture of dissected 3rd instar larva stained with horseradish peroxidase (HRP). The segmental motoneurons emerge from the ventral nerve cord to form neuromuscular junctions (NMJ) as the one framed in white and magnified in **(B). (C-D)** Quantification and corresponding representative images of dissected *zpg*-kd and *dap*-kd 3rd instar larvae stained with HRP and cysteine-string protein (CSP). 2 NMJs per segments 3 to 5 were imaged and presynaptic buttons were counted based on the colocalization of both markers. Scale bars are 30µm. Unpaired two-tailed Student's t-test was performed with n=7 (zpg-kd and dap-kd). Values represent mean ± SEM.

(Figure 3.4A). This behavior is a hallmark of locomotor defects and has been described in several models exhibiting axonal transport deficits (Gindhart et al., 1998; Janssens et al., 2014; Johnson et al., 2013). Morelli et al. (unpublished) therefore studied whether *dacapo* knockdown is responsible for locomotor defects in larvae and adult flies. They have shown that dap-kd 3rd instar larvae exhibit marked alterations in the number of peristaltic movements and crawling speed while adult flies display climbing defects (Figure 3.4B-3.4D). Larvae and adult flies treated with tubastatin showed remarkable improvements in the locomotor behavior (Figure 3.4E-3.4F-3.4G), suggesting that the rescue of microtubule acetylation and transport concomitantly improves locomotion.

Morphological defects of the NMJ such as the number of synaptic buttons can cause locomotor defects in flies (Wise et al., 2013, 2015). Some studies have also shown that some axonal transport defects are correlated with an abnormal NMJ morphology (Liu et al., 2011; Lorenzo et al., 2010). We therefore assessed whether the axonal transport defects exhibited by *dap*-kd larvae were correlated with abnormalities in the number of presynaptic buttons at the NMJ. To this aim, we dissected *zpg*-kd and *dap*-kd larvae following the optimized NMJ dissection protocol (Devireddy et al., 2014; Wu and Luo, 2006) and performed immunostainings using horse radish peroxidase (HRP), a neuronal marker, and cysteine-string protein (CSP), a presynaptic marker (Mao et al., 2014; Xiong et al., 2013) (Figure 3.5A-3.5B). Thus, we demonstrated that the number of synaptic buttons per NMJ was similar between *zpg*-kd and *dap*-kd larvae (Figure 3.5C-3.5D). Consequently, our results show that the integrity of the NMJ morphology is preserved following *dacapo* knockdown despite the existence of underlying axonal transport defects in these larvae. This subsequently suggests that the locomotor defects may be due to synaptic dysfunction and not abnormal synaptic morphology.

4. Discussion

Our results identify dacapo, the p27kip1 fly ortholog, as a modulator of axonal transport velocity through the regulation of microtubule acetylation. Mitochondria and synaptic vesicles labelled with synaptotagmin both exhibited a reduced velocity following dacapo knockdown. The restoration of physiological microtubule acetylation levels by HDAC6 inhibition improved the velocity of mitochondria and synaptic vesicles suggesting a causative link between microtubule acetylation and axonal transport. Dacapo depletion in both larvae and adult flies resulted in locomotor behavior defects that were rescued by HDAC6 inhibition. Increasing the speed of transport in dacapo knockdown animals is therefore associated with an improvement of locomotor activity, suggesting that the axonal transport defect is at least partly responsible for the motor behavior defect. Consistent with this, the morphology of the NMJ was unchanged between control and dacapo knockdown larvae, suggesting that the locomotor behavior defects are not caused by a defect in synaptic morphology but rather a defect in synaptic function.

4.1 Dacapo as a regulator of microtubule acetylation

The rescue of microtubule acetylation by HDAC6 inhibition in dacapo knockdown animal informs on the link between microtubule acetylation and axonal transport that will be discussed later. However, it does not inform on the mechanism through which dacapo modulates microtubule acetylation. Since HDAC6 is the main deacetylase of microtubules, its inhibition increases microtubule acetylation independently of the origin of the defect. I will now discuss how dacapo may modulate microtubule acetylation.

p27 or its fly ortholog dacapo have no reported enzymatic ability to acetylate microtubules. Two hypothesis could explain how the depletion of dacapo results in a reduction of microtubule acetylation levels. First, dacapo depletion could affect microtubule dynamics which may subsequently increase the life-time of microtubules and therefore their acetylation. Second, dacapo could act upstream of tubulin acetyl-transferases and/or deacetylases to regulate their activity and hence modulate microtubule acetylation.

4.1.1 Dacapo could modulate acetylation levels through microtubule stabilization

Acetylation can be used as a marker of stable microtubules as it accumulates stochastically over time in aging microtubules (Li and Yang, 2015). p27 could therefore affect microtubule acetylation through its effect on microtubule dynamics, supported by the ability of p27 to bind to microtubules and promote their polymerization in interneurons (Godin et al., 2012).

p27/dacapo knockdown could therefore induce an increase in microtubule turn over which subsequently reduces their life span and microtubule acetylation. Studying the microtubule

dynamics in dacapo knockdown flies would therefore provide information on the mechanism through which dacapo modulates tubulin acetylation. Some perspectives would be to use available fly lines expressing a +TIP recombinant GFP. End-binding 1 (EB1)-GFP fly lines enable the tracking of microtubule +ends by time-lapse microscopy to assess the proportion of polymerizing microtubules as well as the rate of growth (Ehaideb et al., 2014; Pawson et al., 2009). Detyrosination is another microtubule PTM associated with aging microtubules (Song and Brady, 2015; Webster, 1990). It would therefore be an interesting perspective to perform a co-labeling of acetylation and detyrosination in dacapo knockdown and wild type larvae. A concomitant decrease of tyrosination and acetylation levels would suggest an effect on microtubule stability. Conversely, a decrease in acetylation independently of a change in microtubule tyrosination would suggest a specific modulation of acetylation by dacapo.

4.1.2 Dacapo may act as an upstream regulator of acetyltransferases and/or deacetylases

p27 may enable the transcriptional regulation or stabilization of proteins involved directly or indirectly in microtubule acetylation. Indeed, p27 coordinates neuronal differentiation by stabilizing the transcription factor Neurogenin-2 (Nguyen et al., 2006) and additional roles of p27 as a transcriptional regulator have also been highlighted (Gallastegui et al., 2017; Jeannot et al., 2015). In dacapo knockdown animals, the main enzymes involved in the balance of microtubule acetylation such as αTAT1, αTAT2 and HDAC6 are prime candidates for a regulatory effect of dacapo. The activity of αTAT1 and αTAT2 appears conserved in flies based on preliminary data we collected (Even et al. in preparation). Knockdown of αTAT1 or αTAT2 resulted in a substantial reduction of microtubule acetylation levels while larvae depleted in both αTAT1 and αTAT2 exhibited no detectable acetylated tubulin (Even et al. in preparation). Knockdown of Elp3, the catalytic subunit of the Elongator complex, also resulted in a decrease of microtubule acetylation (Even et al. in preparation), highlighting the conserved role of Elp3 in tubulin acetylation that was originally discovered in C. Elegans and mice (Creppe et al., 2009; Solinger et al., 2010b). Nonetheless, since tubulin acetylation is undetectable in larval motoneurons following αTAT1 and αTAT2 knockout, it is likely that αTAT1 and αTAT2 are the major acetylators in flies. Elp3 may indirectly modulate microtubule acetylation or has a minor role in physiological tubulin acetylation. Comparing the expression and half-life of αTAT1, αTAT2, HDAC6 and Elp3 between wild-type and dacapo knockdown flies may therefore clarify how dacapo regulates microtubule acetylation.

Other proteins involved in the indirect regulation of microtubule acetylation may be putative targets of dacapo. For instance, unpublished interactomic data from Arnaud Besson, collaborator of Laurent Nguyen, highlights an interaction between p27 and the Aurora A kinase.

This kinase phosphorylates HDAC6 to promote its deacetylase activity (Pugacheva et al., 2007). Although Aurora A is conserved in flies (Bell et al., 2015), its role in the modulation of HDAC6 activity has not yet been demonstrated. In human and mouse cancer cells, specific inhibition of Aurora A resulted in an upregulation of p27 expression (Gorgun et al., 2010; Zhou et al., 2015), suggesting that these two proteins have a functional link. It is thus tempting to hypothesize that p27/dacapo maintains physiological levels of acetylation by decreasing HDAC6 phosphorylation through an interaction with Aurora A. Upon loss of p27, Aurora A would phosphorylate HDAC6 more efficiently thus increasing its activity and decreasing microtubule acetylation levels. To explore Aurora A as a downstream target of dacapo, the interaction between dacapo and Aurora A could be confirmed by immuno-precipitations and the expression of Aurora A in dacapo knockdown animals could be assessed by Western Blot and qPCR.

4.2 HDAC6 inhibition may modulate axonal transport independently from increased microtubule acetylation

d'Ydewalle et al., 2011; Dompierre et al., 2007; Godena et al., 2014 and Reed et al., 2006 have previously shown that restoring microtubule acetylation using HDAC6 inhibitors modulates the transport of various cargoes. These studies show that microtubule acetylation levels modulate the number of moving mitochondria as well as the velocity of retrograde bound vesicles transporting brain-derived neurotrophic factor (BDNF), secretory vesicles labelled with vesicular stomatitis virus glycoprotein (VSV-G) and vesicles transporting JIP-1 to dendrites. This suggests a general modulatory effect of microtubule acetylation, also supported by our observation that the velocity of mitochondria and synaptic vesicles is affected by microtubule acetylation levels.

However, HDAC6 is a multifunctional protein with many targets in the cytoplasm (reviewed in Seidel et al., 2015). HDAC6 notably promotes protein clearance by binding to misfolded proteins (Boyault et al., 2006; Lee et al., 2010a), forming aggresomes for autophagy (Lee et al., 2010b; Ouyang et al., 2012) and promoting heat shock protein 90 (HSP90) activity (Kovacs et al., 2005). Since axonal transport defects can arise from protein aggregation (Csizmadia et al., 2008), HDAC6 could exert an effect on transport through its role in protein clearance. Asthana et al., 2013, also showed that pharmacological inhibition of HDAC6 but not genetic depletion resulted in increased microtubule stability. This observation is surprising as both genetic depletion and pharmacological inhibition of HDAC6 increase microtubule acetylation. Asthana et al. show that tubastatin treatment increased HDAC6 binding to microtubules which could explain the shift in microtubule dynamics caused by HDAC6 inhibition. HDAC6 therefore

appears to stabilize microtubules through its MAP activity independently of its ability to deacetylate microtubules.

Although it is becoming clear that HDAC6 inhibition rescues axonal transport defects of various cargos (Chen et al., 2010; d'Ydewalle et al., 2011; Dompierre et al., 2007; Godena et al., 2014; Reed et al., 2006), whether it is due to an increase in microtubule acetylation or another function of HDAC6 can still be debated. Axonal transport may for instance be modulated by HDAC6 inhibition through its effect on microtubule dynamics. Since tubastatin treatment increases HDAC6 binding to microtubules and subsequently microtubule stability (Asthana et al., 2013), axonal transport defects could be rescued independently of increased microtubule acetylation. However, knockdown of HDAC6 and TSA treatment both rescued axonal transport in a *drosophila* model of Parkinson's disease (Godena et al., 2014), suggesting that increased microtubule stabilization by HDAC6 is not necessary to rescue axonal transport. Genetic inhibition of HDAC6 in our *drosophila* model would clarify whether HDAC6 MAP activity plays a part in the rescue phenotype we observe.

In order to strengthen the link between microtubule acetylation and transport, an interesting perspective would be to rescue the acetylation levels using αTAT1 overexpression since this enzyme displays high substrate specificity for tubulin (Kalebic et al., 2013; Shida et al., 2010). This approach would exclude confounding factors concomitant to the inhibition of the multifunctional deacetylase HDAC6.

4.3 Mechanisms coupling microtubule acetylation to transport kinetics

A mechanistic link between microtubule acetylation and axonal transport has been argued in several studies despite the confounding factors induced by the use of HDAC6 inhibitors. A mechanism identified by Reed et al. proposes that increasing microtubule acetylation subsequently enhances the binding and motility of the kinesin-1 family while Dompierre et al. have shown that increased microtubule acetylation is associated with enhanced recruitment and binding of kinesin-1, dynactin and cytoplasmic dynein. Since dynein and dynactin drive the retrograde transport of all cargos, the velocity of synaptic vesicles and mitochondria may be affected by microtubule acetylation levels through the recruitment of the dynein/dynactin complex. On the other hand, the anterograde transport of mitochondria transport critically relies on the kinesin-1 family including KIF5A (Campbell et al., 2014), KIF5B (Tanaka et al., 1998) and KIF5C (Kanai et al., 2000) and is only partially reliant on KIF1Bα of the kinesin-3 family (Nangaku et al., 1994). However, the anterograde transport of synaptic vesicles delivering synaptotagmin depends on KIF1A, a kinesin isotype of the kinesin-3 family (Lo et al., 2011; Okada et al., 1995). The mechanism identified by Reed et al. and Dompierre et al. could thus

explain how microtubule acetylation modulates the transport kinetics of mitochondria. Nevertheless, the anterograde transport of synaptic vesicles relies on KIF1A and not the kinesin-1 family, thus suggesting that additional mechanisms through which microtubule acetylation modulates anterograde transport are in play. For instance, the enhanced binding and motility of kinesin-1 on acetylated microtubules may be generalized to other kinesin families since the structure of the microtubule binding domain is highly conserved between kinesin families (Hirokawa and Noda, 2008). Studying the binding affinity of other kinesin families on non-acetylated and acetylated microtubules *in vitro* would clarify whether this mechanism is generalized to other kinesin families.

Another mechanism linking microtubule acetylation to the modulation of transport was described by Godena et al., 2014. They show that a LRRK2 mutant, a common genetic cause of Parkinson's disease, preferentially associates with poorly acetylated microtubules and inhibits axonal transport. Increasing microtubule acetylation with HDAC6 inhibitors subsequently prevented the association of mutant LRRK2 with microtubules and rescued the transport defects (Godena et al., 2014). Microtubule acetylation can therefore regulate the affinity of MAPs such as LRRK2 and motors such as kinesin-1 or dynein to modulate transport. Microtubule structure has been shown to affect kinesin binding in several studies (Krebs et al., 2004; Skiniotis et al., 2004). It is thus tempting to hypothesize that microtubule acetylation induces conformational changes in α-tubulin which in turn modulates the affinity of MAPs and motors. However, a recent study has shown that the architecture of microtubules and the conformation of tubulin are unaltered by the acetylation of microtubules *in vitro* (Howes et al., 2014). This suggests that microtubule acetylation may only have a local effect on the microtubule lumen where Lys-40 acetylation occurs through the recognition of modified Lys-40 by intra luminal proteins (Howes et al., 2014).

Studies have shown that microtubules display luminal globular particles with a diameter of 6nm which are mostly juxtaposed to the microtubules walls (Bouchet-Marquis et al., 2007; Garvalov et al., 2006). This particle size is in the same order of magnitude displayed by large globular proteins (Erickson, 2009). In *C. Elegans*, mutations in MEC-17, the main tubulin acetyl-transferase, resulted in a complete disappearance of the luminal material (Topalidou et al., 2012). Although the identity of these particles is unknown, this observation suggests that acetylation is required for their presence and raises the hypothesis that these particles are MAPs that may regulate different aspects of microtubule function. Microtubule acetylation could therefore exert its functions by regulating the affinity of luminal MAPs which subsequently modulates the affinity of motors or other MAPs with microtubules. This exciting field of research is however impaired by the ability to distinguish MAPs associated with the lumen or

microtubule lattice. New methods to identify the nature of the luminal particles are therefore required in order to explore this attractive hypothesis.

4.4 Locomotor behavior defects and axonal transport

Locomotor behavior defects are a hallmark of neurodegenerative diseases such as Parkinson's disease, ALS or Charcot-Marie-Tooth. Some studies have shown that axonal transport defects can result in motor defects (Godena et al., 2014; Janssens et al., 2014) and consistent with this data, we found that dacapo knockdown results in locomotor defects in addition to impairing axonal transport. Axonal transport is crucial for the development of the neuronal circuitry due to its role in providing energy and material for synaptogenesis (Goldstein et al., 2008). However, we did not observe abnormalities in synaptic morphology at the NMJ of 3rd instar larvae. The slowdown of transport exhibited in dacapo knockdown larvae may only arise after a specific developmental stage posterior to presynaptic button formation or the defect may not be grave enough to induce morphological changes.

The locomotor behavior defect was nonetheless rescued by acute HDAC6 inhibition which suggests a causative link with axonal transport independent of morphological changes. Instead, physiological axonal transport may be required to provide the neurotransmitters and energy necessary to ensure proper synaptic function in larvae. The fact that motor behavior was restored with a 30min tubastatin treatment is highly suggestive of a fast restoration of synaptic function through appropriate supply of proteins and energy. Electrophysiological analysis at the NMJ could be performed to shed light on the mechanism by which dacapo knockdown induces locomotor behavior defects. Electrophysiological methods to assess synaptic function are well developed for dissected *drosophila* larvae (Imlach and McCabe, 2009) and have been used in numerous studies (Jepson et al., 2014; Staples and Broadie, 2013). Of particular interest, a *drosophila* model of amyotrophic lateral sclerosis (ALS) with TAR DNA binding protein homolog (TBPH) overexpression exhibits axonal transport defects (Baldwin et al., 2016). Diaper et al., 2013 have shown that brain-specific overexpression of TBPH induces locomotor behavior defects with unaltered synaptic morphology. Instead, the amplitude and frequency of excitatory junction potentials was impaired, likely causing the motor defects (Diaper et al., 2013).

4.5 Axonal transport and microtubule acetylation in neurodegenerative diseases

Axonal transport is an essential process for the maintenance and function of neurons and as such, many axonal transport defects have been pinpointed in neurodegenerative disorders (reviewed in Millecamps and Julien, 2013) and malformations of cortical development (Poirier

et al., 2013). The defects observed may play a causative role in the genesis of the disease but they may also reflect the distressed cellular homeostasis. In some instances, mutations in motors or MAPs have been highlighted, which strongly supports a causative link between axonal transport and the emergence of the disorder (Harms et al., 2012; Poirier et al., 2013). Abnormal microtubule acetylation levels are also displayed in some neurodegenerative diseases models and are correlated with axonal transport defects. Restoring microtubule acetylation in a Parkinson's or Huntington's disease model rescues axonal transport (d'Ydewalle et al., 2011; Dompierre et al., 2007; Godena et al., 2014) while in a Charcot-Marie-Tooth model, rescuing axonal transport also alleviated motor symptoms (d'Ydewalle et al., 2011). Following this study, Kim et al., 2016 utilized induced pluripotent stem cells derived from patients suffering from Charcot-Marie-Tooth disease to study the link between microtubule acetylation and axonal transport defects. They show that the cultured motoneurons display reduced levels of microtubule acetylation and defective axonal transport of mitochondria. Consistent with our results and the previous literature, HDAC6 inhibitors restored acetylation levels and rescued mitochondria transport velocity.

Of interest, p27 expression is reduced in a mouse model of ALS but also at the mRNA level in human patients suffering from ALS (Cova et al., 2010; Jensen et al., 2016). A better understanding of the regulation of microtubule acetylation as well as the mechanisms through which this PTM modulates transport will provide key insights for the treatment of some neurodegenerative diseases.

5. Abbreviations

αTAT1 : alpha-tubulin N-acetyltransferase 1

αTAT2 : alpha-tubulin N-acetyltransferase 2

ALS : Amyotrophic lateral sclerosis

BDNF : Brain-derived neurotrophic factor

BSA: Bovine serum albumin

CDK : Cyclin-dependent kinase HDAC6 : Histone deacetylase 6

CLASP2 : CLIP-associating protein 2

CNS : Central nervous system

CSP : Cysteine string protein

DMSO : Dimethyl sulfoxide

EB1 : End-binding 1

Elp3 : Elongator complex protein 3

GFP : Green fluorescent protein

HRP: Horse raddish peroxidase

HSP90 : Heat shock protein 90

JIP1 : JNK-interacting protein 1

LRRK2 : Leucine-rich repeat kinase 2

Lys40 : Lysine 40

MAP : Microtubule associated protein

NMJ : Neuromuscular junction

PTMs : Post-translational modifications

SIRT2 : Sirtuin 2

TBPH : TAR DNA binding protein homology

UAS : Upstream activating sequence

VNC : Ventral nerve cord

VSV-G : Vesicular stomatitis virus glycoprotein

ZPG : Zero population growth

+TIPs : Plus-end interacting proteins

6. Contributions and supplementary figure

The project I worked on was collaborative and implicated shared efforts.

- I carried out the mitochondria transport experiments including the recordings and analysis
- Axonal transport of synaptotagmin was carried out by Giovanni Morelli
- I carried out the dissections and immunohistochemistry experiments for the microtubule acetylation and NMJ experiments. Imaging and analysis were mostly performed by Giovanni Morelli
- Locomotor Behavior experiments were performed by Giovanni Morelli

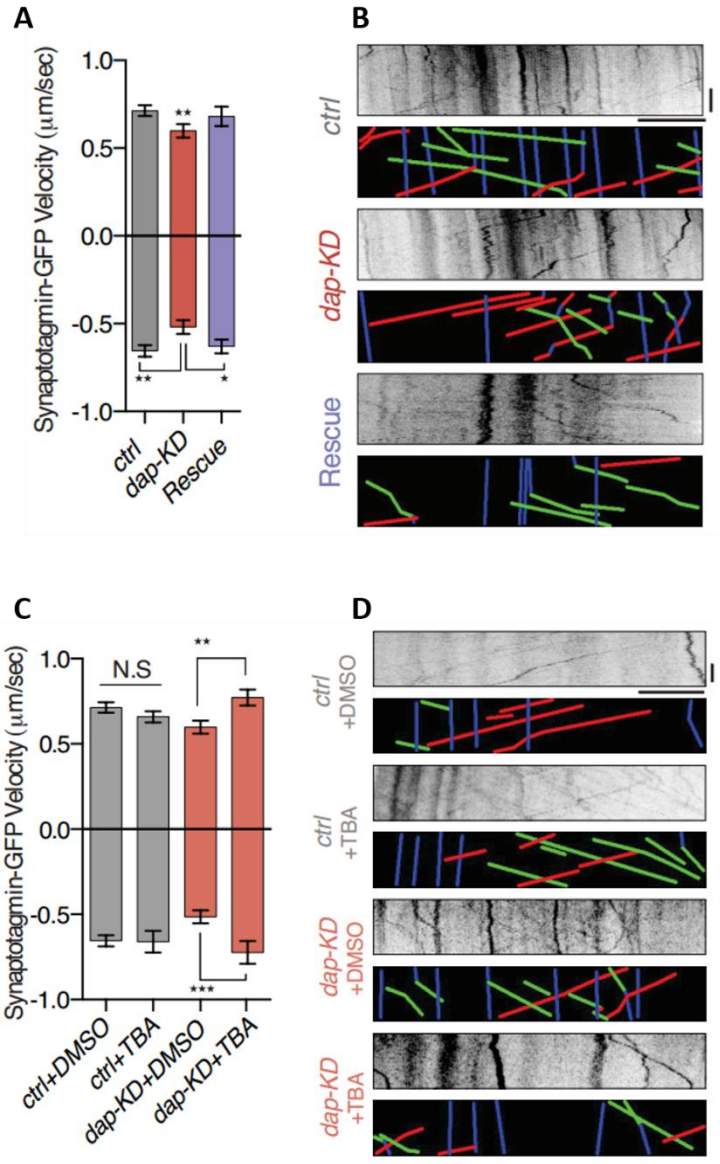

Supplementary figure 3.1: *dacapo* knockdown slows down synaptic vesicle transport
(A-C) Quantification of synaptic vesicles velocity based on live-imaging of synaptotagmin-GFP larvae. Positive and negative values represent anterograde and retrograde movement respectively. **(C-D)** *zpg*-kd and *dap*-kd larvae fed for 30min with either 1mM DMSO or tubastatin A (TBA) sucrose solution. **(A-C)** Values are mean ± standard error of the mean and were analyzed using the non-parametric Kruskal-Wallis test followed by Dunn post hoc-tests. *p<0.5, **p<0,01, ***p<0,001. N (of mitochondria) is > 50 with at least 5 animals per condition. **(A)** N for vesicles > 200; N for animals = 20 (control), 22 (*dap*-kd), 15 (Rescue). **(C)** N for vesicles > 150; N for animals = 10 (ctrl + DMSO), 10 (ctrl + TBA), 9 (*dap*-kd + DMSO), 8 (*dap*-kd + TBA). **(D)** Representative kymographs and their corresponding colored kymographs. Green, red and blue line

7. Bibliography

Akella, J.S., Wloga, D., Kim, J., Starostina, N.G., Lyons-Abbott, S., Morrissette, N.S., Dougan, S.T., Kipreos, E.T., and Gaertig, J. (2010). MEC-17 is an α-tubulin acetyltransferase. Nature *467*, 218–222.

Akhmanova, A., and Steinmetz, M.O. (2008). Tracking the ends: a dynamic protein network controls the fate of microtubule tips. Nat. Rev. Mol. Cell Biol. *9*, 309–322.

Akhmanova, A., and Steinmetz, M.O. (2015). Control of microtubule organization and dynamics: two ends in the limelight. Nat. Rev. Mol. Cell Biol. *16*, 711–726.

Alushin, G.M., Lander, G.C., Kellogg, E.H., Zhang, R., Baker, D., and Nogales, E. (2014). High-Resolution Microtubule Structures Reveal the Structural Transitions in αβ-Tubulin upon GTP Hydrolysis. Cell *157*, 1117–1129.

Asthana, J., Kapoor, S., Mohan, R., and Panda, D. (2013). Inhibition of HDAC6 Deacetylase Activity Increases Its Binding with Microtubules and Suppresses Microtubule Dynamic Instability in MCF-7 Cells. J. Biol. Chem. *288*, 22516–22526.

Baldassarre, G., Belletti, B., Nicoloso, M.S., Schiappacassi, M., Vecchione, A., Spessotto, P., Morrione, A., Canzonieri, V., and Colombatti, A. (2005). p27Kip1-stathmin interaction influences sarcoma cell migration and invasion. Cancer Cell *7*, 51–63.

Baldwin, K.R., Godena, V.K., Hewitt, V.L., and Whitworth, A.J. (2016). Axonal transport defects are a common phenotype in Drosophila models of ALS. Hum. Mol. Genet. ddw105.

Basu, S., Sladecek, S., Martinez de la Pena y Valenzuela, I., Akaaboune, M., Smal, I., Martin, K., Galjart, N., and Brenner, H.R. (2015). CLASP2-dependent microtubule capture at the neuromuscular junction membrane requires LL5 and actin for focal delivery of acetylcholine receptor vesicles. Mol. Biol. Cell *26*, 938–951.

Bell, G.P., Fletcher, G.C., Brain, R., and Thompson, B.J. (2015). Aurora Kinases Phosphorylate Lgl to Induce Mitotic Spindle Orientation in Drosophila Epithelia. Curr. Biol. *25*, 61–68.

Belmadani, S., Poüs, C., Fischmeister, R., and Méry, P.F. (2004). Post-translational modifications of tubulin and microtubule stability in adult rat ventricular myocytes and immortalized HL-1 cardiomyocytes. Mol. Cell. Biochem. *258*, 35–48.

Bencivenga, D., Caldarelli, I., Stampone, E., Mancini, F.P., Balestrieri, M.L., Della Ragione, F., and Borriello, A. (2017). p27 Kip1 and human cancers: A reappraisal of a still enigmatic protein. Cancer Lett.

Berni, J., Pulver, S.R., Griffith, L.C., and Bate, M. (2012). Autonomous circuitry for substrate exploration in freely moving drosophila larvae. Curr. Biol. *22*, 1861–1870.

Besson, A., Dowdy, S.F., and Roberts, J.M. (2008). CDK Inhibitors: Cell Cycle Regulators and Beyond. Dev. Cell *14*, 159–169.

Bhagwat, S., Dalvi, V., Chandrasekhar, D., Matthew, T., Acharya, K., Gajbhiye, R., Kulkarni, V., Sonawane, S., Ghosalkar, M., and Parte, P. (2014). Acetylated α-tubulin is reduced in individuals with poor sperm motility. Fertil. Steril. *101*, 95–104.e3.

Bienkiewicz, E.A., Adkins, J.N., and Lumb, K.J. (2002). Functional Consequences of Preorganized Helical Structure in the Intrinsically Disordered Cell-Cycle Inhibitor p27 Kip1 †. Biochemistry *41*, 752–759.

Bouchet-Marquis, C., Zuber, B., Glynn, A.-M., Eltsov, M., Grabenbauer, M., Goldie, K.N., Thomas, D., Frangakis, A.S., Dubochet, J., and Chrétien, D. (2007). Visualization of cell microtubules in their native state. Biol. Cell *99*, 45–53.

Boyault, C., Gilquin, B., Zhang, Y., Rybin, V., Garman, E., Meyer-Klaucke, W., Matthias, P., Müller, C.W., and Khochbin, S. (2006). HDAC6–p97/VCP controlled polyubiquitin chain turnover. EMBO J. *25*, 3357–3366.

Brand, A.H., and Perrimon, N. (1993). Targeted gene expression as a means of altering cell fates and generating dominant phenotypes. Development *118*, 401–415.

Brent, J., Werner, K., and McCabe, B.D. (2009). Drosophila larval NMJ immunohistochemistry. J. Vis. Exp. 4–5.

Butler, K. V, Kalin, J., Brochier, C., Vistoli, G., Langley, B., and Kozikowski, A.P. (2010). Rational Design and Simple Chemistry Yield a Superior, Neuroprotective HDAC6 Inhibitor, Tubastatin A. J. Am. Chem. Soc. *132*, 10842–10846.

Cambray-Deakin, M.A., and Burgoyne, R.D. (1987). Posttranslational modifications of α-tubulin: Acetylated and detyrosinated forms in axons of rat cerebellum. J. Cell Biol. *104*, 1569–1574.

Campbell, P.D., Shen, K., Sapio, M.R., Glenn, T.D., Talbot, W.S., and Marlow, F.L. (2014). Unique Function of

Kinesin Kif5A in Localization of Mitochondria in Axons. J. Neurosci. *34*, 14717–14732.

Cardona, A., Larsen, C., and Hartenstein, V. (2009). Neuronal fiber tracts connecting the brain and ventral nerve cord of the early Drosophila larva. J. Comp. Neurol. *515*, 427–440.

Carlier, M.F., and Pantaloni, D. (1981). Kinetic analysis of guanosine 5'-triphosphate hydrolysis associated with tubulin polymerization. Biochemistry *20*, 1918–1924.

Chen, P.B., Hung, J.-H., Hickman, T.L., Coles, A.H., Carey, J.F., Weng, Z., Chu, F., and Fazzio, T.G. (2013). Hdac6 regulates Tip60-p400 function in stem cells. Elife *2*.

Chen, S., Owens, G.C., Makarenkova, H., and Edelman, D.B. (2010). HDAC6 Regulates Mitochondrial Transport in Hippocampal Neurons. PLoS One *5*, e10848.

Clément, O., Hemming, I.A., Gladwyn-Ng, I.E., Qu, Z., Li, S.S., Piper, M., and Heng, J.I.-T. (2017). Rp58 and p27(kip1) coordinate cell cycle exit and neuronal migration within the embryonic mouse cerebral cortex. Neural Dev. *12*, 8.

Colonques, J., Ceron, J., Reichert, H., and Tejedor, F.J. (2011). A transient expression of prospero promotes cell cycle exit of drosophila postembryonic neurons through the regulation of Dacapo. PLoS One *6*.

Conacci-Sorrell, M., Ngouenet, C., and Eisenman, R.N. (2010). Myc-nick: A cytoplasmic cleavage product of Myc that promotes α-tubulin acetylation and cell differentiation. Cell *142*, 480–493.

Conde, C., and Cáceres, A. (2009). Microtubule assembly, organization and dynamics in axons and dendrites. Nat. Rev. Neurosci. *10*, 319–332.

Cova, E., Ghiroldi, A., Guareschi, S., Mazzini, G., Gagliardi, S., Davin, A., Bianchi, M., Ceroni, M., and Cereda, C. (2010). G93A SOD1 alters cell cycle in a cellular model of Amyotrophic Lateral Sclerosis. Cell. Signal. *22*, 1477–1484.

Cragnaz, L., Klima, R., De Conti, L., Romano, G., Feiguin, F., Buratti, E., Baralle, M., and Baralle, F.E. (2015). An age-related reduction of brain TBPH/TDP-43 levels precedes the onset of locomotion defects in a Drosophila ALS model. Neuroscience *311*, 415–421.

Creppe, C., Malinouskaya, L., Volvert, M.L., Gillard, M., Close, P., Malaise, O., Laguesse, S., Cornez, I., Rahmouni, S., Ormenese, S., et al. (2009). Elongator Controls the Migration and Differentiation of Cortical Neurons through Acetylation of α-Tubulin. Cell *136*, 551–564.

Csizmadia, V., Raczynski, A., Csizmadia, E., Fedyk, E.R., Rottman, J., and Alden, C.L. (2008). Effect of an experimental proteasome inhibitor on the cytoskeleton, cytosolic protein turnover, and induction in the neuronal cells in vitro. Neurotoxicology *29*, 232–243.

d'Ydewalle, C., Krishnan, J., Chiheb, D.M., Van Damme, P., Irobi, J., Kozikowski, A.P., Berghe, P. Vanden, Timmerman, V., Robberecht, W., and Van Den Bosch, L. (2011). HDAC6 inhibitors reverse axonal loss in a mouse model of mutant HSPB1–induced Charcot-Marie-Tooth disease. Nat. Med. *17*, 968–974.

Desai, A., and Mitchison, T.J. (1997). Microtubule Polymerization Dynamics. Annu. Rev. Cell Dev. Biol. *13*, 83–117.

Devireddy, S., Sung, H., Liao, P.C., Garland-Kuntz, E., and Hollenbeck, P.J. (2014). Analysis of mitochondrial traffic in drosophila (Elsevier Inc.).

Diaper, D.C., Adachi, Y., Sutcliffe, B., Humphrey, D.M., Elliott, C.J.H., Stepto, A., Ludlow, Z.N., Vanden Broeck, L., Callaerts, P., Dermaut, B., et al. (2013). Loss and gain of Drosophila TDP-43 impair synaptic efficacy and motor control leading to age-related neurodegeneration by loss-of-function phenotypes. Hum. Mol. Genet. *22*, 1539–1557.

Dompierre, J.P., Godin, J.D., Charrin, B.C., Cordelières, F.P., King, S.J., Humbert, S., and Saudou, F. (2007). Histone deacetylase 6 inhibition compensates for the transport deficit in Huntington's disease by increasing tubulin acetylation. J. Neurosci. *27*, 3571–3583.

Duffy, J.B. (2002). GAL4 system indrosophila: A fly geneticist's swiss army knife. Genesis *34*, 1–15.

Ehaideb, S.N., Iyengar, A., Ueda, A., Iacobucci, G.J., Cranston, C., Bassuk, A.G., Gubb, D., Axelrod, J.D., Gunawardena, S., Wu, C.-F., et al. (2014). Prickle Modulates Microtubule Polarity and Axonal Transport To Ameliorate Seizures in Flies. Proc. Natl. Acad. Sci. *111*, 11187–11192.

Erickson, H.P. (2009). Size and Shape of Protein Molecules at the Nanometer Level Determined by Sedimentation, Gel Filtration, and Electron Microscopy. Biol. Proced. Online *11*, 32–51.

Gallastegui, E., Biçer, A., Orlando, S., Besson, A., Pujol, M.J., and Bachs, O. (2017). p27Kip1 represses the Pitx2-mediated expression of p21Cip1 and regulates DNA replication during cell cycle progression. Oncogene *36*, 350–361.

Garner, J. a, and Lasek, R.J. (1982). Cohesive axonal transport of the slow component b complex of polypeptides. J. Neurosci. *2*, 1824–1835.

Garvalov, B.K., Zuber, B., Bouchet-Marquis, C., Kudryashev, M., Gruska, M., Beck, M., Leis, A., Frischknecht, F., Bradke, F., Baumeister, W., et al. (2006). Luminal particles within cellular microtubules. J. Cell Biol. *174*, 759–765.

Gindhart, J.G., Desai, C.J., Beushausen, S., Zinn, K., and Goldstein, L.S.B. (1998). Kinesin light chains are essential for axonal transport in Drosophila. J. Cell Biol. *141*, 443–454.

Godena, V.K., Brookes-Hocking, N., Moller, A., Shaw, G., Oswald, M., Sancho, R.M., Miller, C.C.J., Whitworth, A.J., and De Vos, K.J. (2014). Increasing microtubule acetylation rescues axonal transport and locomotor deficits caused by LRRK2 Roc-COR domain mutations. Nat. Commun. *5*, 5245.

Godin, J.D., and Nguyen, L. (2014). Novel Functions of Core Cell Cycle Regulators in Neuronal Migration. Adv. Exp. Med. Biol. *800*, 97–111.

Godin, J.D., Thomas, N., Laguesse, S., Malinouskaya, L., Close, P., Malaise, O., Purnelle, A., Raineteau, O., Campbell, K., Fero, M., et al. (2012). P27Kip1 Is a Microtubule-Associated Protein that Promotes Microtubule Polymerization during Neuron Migration. Dev. Cell *23*, 729–744.

Goldstein, A.Y., Wang, X., and Schwarz, T.L. (2008). Axonal transport and the delivery of pre-synaptic components. Curr. Opin. Neurobiol. *18*, 495–503.

Gorgun, G., Calabrese, E., Hideshima, T., Ecsedy, J., Perrone, G., Mani, M., Ikeda, H., Bianchi, G., Hu, Y., Cirstea, D., et al. (2010). A novel Aurora-A kinase inhibitor MLN8237 induces cytotoxicity and cell-cycle arrest in multiple myeloma. Blood *115*, 5202–5213.

Greenspan, R.J. (1997). Fly Pushing: The Theory and Practice of Drosophila genetics (Plain-view, New York).

Griffin, J.W., Price, D.L., Drachman, D.B., and Engel, W.K. (1976). Axonal transport to and from the motor nerve ending. Ann. New York Acad. Sci. *274*, 31–45.

Gupta, A., Tsai, L.-H., and Wynshaw-Boris, A. (2002). Life Is a Journey: a Genetic Look At Neocortical Development. Nat. Rev. Genet. *3*, 342–355.

Hales, K.G., Korey, C.A., Larracuente, A.M., and Roberts, D.M. (2015a). Genetics on the Fly: A Primer on the Drosophila Model System. Genetics *201*, 815–842.

Hales, K.G., Korey, C.A., Larracuente, A.M., and Roberts, D.M. (2015b). Genetics on the fly: A primer on the drosophila model system. Genetics *201*, 815–842.

Harms, M.B., Ori-McKenney, K.M., Scoto, M., Tuck, E.P., Bell, S., Ma, D., Masi, S., Allred, P., Al-Lozi, M., Reilly, M.M., et al. (2012). Mutations in the tail domain of DYNC1H1 cause dominant spinal muscular atrophy. Neurology *78*, 1714–1720.

Harting, K., and Knöll, B. (2010). SIRT2-mediated protein deacetylation: An emerging key regulator in brain physiology and pathology. Eur. J. Cell Biol. *89*, 262–269.

Hirokawa, N., and Noda, Y. (2008). Intracellular Transport and Kinesin Superfamily Proteins : Structure Dynamics and Function. Physiol. Rev. *88*, 1089–1118.

Hirokawa, N., Satoyoshitake, R., Kobayashi, N., Pfister, K.K., Bloom, G.S., and Brady, S.T. (1991). Kinesin Associates with Anterogradely Transported Membranous Organelles In Vivo. J. Cell Biol. *114*, 295–302.

Horiuchi, D., Barkus, R. V., Pilling, A.D., Gassman, A., and Saxton, W.M. (2005). APLIP1, a kinesin binding JIP-1/JNK scaffold protein, influences the axonal transport of both vesicles and mitochondria in Drosophila. Curr. Biol. *15*, 2137–2141.

Howes, S.C., Alushin, G.M., Shida, T., Nachury, M. V, and Nogales, E. (2014). Effects of tubulin acetylation and tubulin acetyltransferase binding on microtubule structure. Mol. Biol. Cell *25*, 257–266.

Hubbert, C., Guardiola, A., Shao, R., Kawaguchi, Y., Ito, A., Nixon, A., Yoshida, M., Wang, X.-F., and Yao, T.-P. (2002). HDAC6 is a microtubule-associated deacetylase. Nature *417*, 455–458.

Imlach, W., and McCabe, B.D. (2009). Electrophysiological Methods for Recording Synaptic Potentials from the NMJ of Drosophila Larvae. J. Vis. Exp.

Itoh, Y., Masuyama, N., Nakayama, K., Nakayama, K.I., and Gotoh, Y. (2007). The Cyclin-dependent Kinase Inhibitors p57 and p27 Regulate Neuronal Migration in the Developing Mouse Neocortex. J. Biol. Chem. *282*, 390–396.

Janke, C. (2014). The tubulin code: Molecular components, readout mechanisms, functions. J. Cell Biol. *206*, 461–472.

Janke, C., and Chloë Bulinski, J. (2011). Post-translational regulation of the microtubule cytoskeleton: mechanisms and functions. Nat. Rev. Mol. Cell Biol. *12*, 773–786.

Janssens, K., Goethals, S., Atkinson, D., Ermanoska, B., Fransen, E., Jordanova, A., Auer-Grumbach, M., Asselbergh, B., and Timmerman, V. (2014). Human Rab7 mutation mimics features of Charcot-Marie-Tooth neuropathy type 2B in drosophila. Neurobiol. Dis. *65*, 211–219.

Jeannot, P., Callot, C., Baer, R., Duquesnes, N., Guerra, C., Guillermet-Guibert, J., Bachs, O., and Besson, A. (2015). Loss of p27Kip1 promotes metaplasia in the pancreas via the regulation of Sox9 expression. Oncotarget.

Jensen, L., Jørgensen, L.H., Bech, R.D., Frandsen, U., and Schrøder, H.D. (2016). Skeletal Muscle Remodelling as a Function of Disease Progression in Amyotrophic Lateral Sclerosis. Biomed Res. Int. *2016*, 1–12.

Jepson, J.E.C., Shahidullah, M., Liu, D., le Marchand, S.J., Liu, S., Wu, M.N., Levitan, I.B., Dalva, M.B., and Koh, K. (2014). Regulation of synaptic development and function by the Drosophila PDZ protein Dyschronic. Development *141*, 4548–4557.

Johnson, A.A., Sarthi, J., Pirooznia, S.K., Reube, W., and Elefant, F. (2013). Increasing Tip60 HAT Levels Rescues Axonal Transport Defects and Associated Behavioral Phenotypes in a Drosophila Alzheimer's Disease Model. J. Neurosci. *33*, 7535–7547.

Johnson, E.L., Fetter, R.D., and Davis, G.W. (2009). Negative Regulation of Active Zone Assembly by a Newly Identified SR Protein Kinase. PLoS Biol. *7*, e1000193.

Kalebic, N., Sorrentino, S., Perlas, E., Bolasco, G., Martinez, C., and Heppenstall, P.A. (2013). αTAT1 is the major α-tubulin acetyltransferase in mice. Nat. Commun. *4*.

Kanai, Y., Okada, Y., Tanaka, Y., Harada, A., Terada, S., and Hirokawa, N. (2000). KIF5C, a Novel Neuronal Kinesin Enriched in Motor Neurons. J. Neurosci. *20*, 6374–6384.

Kim, G.W., Li, L., Gorbani, M., You, L., and Yang, X.J. (2013). Mice lacking alpha-tubulin acetyltransferase 1 are viable but display alpha-tubulin acetylation deficiency and dentate gyrus distortion. J. Biol. Chem. *288*, 20334–20350.

Kim, J.-Y., Woo, S.-Y., Hong, Y. Bin, Choi, H., Kim, J., Choi, H., Mook-Jung, I., Ha, N., Kyung, J., Koo, S.K., et al. (2016). HDAC6 Inhibitors Rescued the Defective Axonal Mitochondrial Movement in Motor Neurons Derived from the Induced Pluripotent Stem Cells of Peripheral Neuropathy Patients with HSPB1 Mutation. Stem Cells Int. *2016*, 1–14.

Kovacs, J.J., Murphy, P.J.M., Gaillard, S., Zhao, X., Wu, J.-T., Nicchitta, C. V., Yoshida, M., Toft, D.O., Pratt, W.B., and Yao, T.-P. (2005). HDAC6 Regulates Hsp90 Acetylation and Chaperone-Dependent Activation of Glucocorticoid Receptor. Mol. Cell *18*, 601–607.

Krebs, A., Goldie, K.N., and Hoenger, A. (2004). Complex Formation with Kinesin Motor Domains Affects the Structure of Microtubules. J. Mol. Biol. *335*, 139–153.

Lacy, E.R., Filippov, I., Lewis, W.S., Otieno, S., Xiao, L., Weiss, S., Hengst, L., and Kriwacki, R.W. (2004). p27 binds cyclin–CDK complexes through a sequential mechanism involving binding-induced protein folding. Nat. Struct. Mol. Biol. *11*, 358–364.

Lane, M.E., Sauer, K., Wallace, K., Jan, Y.N., Lehner, C.F., and Vaessin, H. (1996). Dacapo, a cyclin-dependent kinase inhibitor, stops cell proliferation during Drosophila development. Cell *87*, 1225–1235.

Lanson, N.A., Maltare, A., King, H., Smith, R., Kim, J.H., Taylor, J.P., Lloyd, T.E., and Pandey, U.B. (2011). A Drosophila model of FUS-related neurodegeneration reveals genetic interaction between FUS and TDP-43. Hum. Mol. Genet. *20*, 2510–2523.

Lee, J.-Y., Nagano, Y., Taylor, J.P., Lim, K.L., and Yao, T.-P. (2010a). Disease-causing mutations in Parkin impair mitochondrial ubiquitination, aggregation, and HDAC6-dependent mitophagy. J. Cell Biol. *189*, 671–679.

Lee, J.-Y., Koga, H., Kawaguchi, Y., Tang, W., Wong, E., Gao, Y.-S., Pandey, U.B., Kaushik, S., Tresse, E., Lu, J., et al. (2010b). HDAC6 controls autophagosome maturation essential for ubiquitin-selective quality-control autophagy. EMBO J. *29*, 969–980.

Lessing, D., and Bonini, N.M. (2009). Maintaining the brain: insight into human neurodegeneration from Drosophila melanogaster mutants. Nat. Rev. Genet. *10*, 359–370.

Li, L., and Yang, X.J. (2015). Tubulin acetylation: Responsible enzymes, biological functions and human diseases. Cell. Mol. Life Sci. *72*, 4237–4255.

Little, M., and Seehaus, T. (1988). Comparative analysis of tubulin sequences. Comp. Biochem. Physiol. -- Part B Biochem. *90*, 655–670.

Liu, Z., Huang, Y., Zhang, Y., Chen, D., and Zhang, Y.Q. (2011). Drosophila Acyl-CoA synthetase long-chain

family member 4 regulates axonal transport of synaptic vesicles and is required for synaptic development and transmission. J. Neurosci. *31*, 2052–2063.

Lo, K.W.-H., Kan, H.-M., and Pfister, K.K. (2006). Identification of a Novel Region of the Cytoplasmic Dynein Intermediate Chain Important for Dimerization in the Absence of the Light Chains. J. Biol. Chem. *281*, 9552–9559.

Lo, K.Y., Kuzmin, A., Unger, S.M., Petersen, J.D., and Silverman, M.A. (2011). KIF1A is the primary anterograde motor protein required for the axonal transport of dense-core vesicles in cultured hippocampal neurons. Neurosci. Lett. *491*, 168–173.

Lorenzo, D.N., Li, M.G., Mische, S.E., Armbrust, K.R., Ronum, L.P.W., and Hays, T.S. (2010). Spectrin mutations that cause spinocerebellar ataxia type 5 impair axonal transport and induce neurodegeneration in Dmsophila. J. Cell Biol. *189*, 143–158.

Ludueuna, R.F. (1993). Are Tubulin Isotypes Functionally Significant. Mol. Biol. Cell *4*, 445–457.

Maday, S., Twelvetrees, A.E., Moughamian, A.J., and Holzbaur, E.L.F. (2014). Axonal Transport: Cargo-Specific Mechanisms of Motility and Regulation. Neuron *84*, 292–309.

Mao, C.-X., Xiong, Y., Xiong, Z., Wang, Q., Zhang, Y.Q., and Jin, S. (2014). Microtubule-severing protein Katanin regulates neuromuscular junction development and dendritic elaboration in Drosophila. Development *141*, 1064–1074.

McGurk, L., Berson, A., and Bonini, N.M. (2015). Drosophila as an In Vivo Model for Human Neurodegenerative Disease. Genetics *201*, 377–402.

Medioni, C., Ephrussi, A., and Besse, F. (2015). Live imaging of axonal transport in Drosophila pupal brain explants. Nat. Protoc. *10*, 574–584.

Meyer, C.A., Kramer, I., Dittrich, R., Marzodko, S., Emmerich, J., and Lehner, C.F. (2002). Drosophila p27Dacapo expression during embryogenesis is controlled by a complex regulatory region independent of cell cycle progression. Development *129*, 319–328.

Miki, H., Setou, M., Kaneshiro, K., and Hirokawa, N. (2001). All kinesin superfamily protein, KI, genes in mouse and human. Proc. Natl. Acad. Sci. U. S. A. *98*, 7004–7011.

Millecamps, S., and Julien, J.-P. (2013). Axonal transport deficits and neurodegenerative diseases. Nat. Rev. Neurosci. *14*, 161–176.

Mitchell, D.J., Blasier, K.R., Jeffery, E.D., Ross, M.W., Pullikuth, A.K., Suo, D., Park, J., Smiley, W.R., Lo, K.W.-H., Shabanowitz, J., et al. (2012). Trk Activation of the ERK1/2 Kinase Pathway Stimulates Intermediate Chain Phosphorylation and Recruits Cytoplasmic Dynein to Signaling Endosomes for Retrograde Axonal Transport. J. Neurosci. *32*, 15495–15510.

Mitchison, T., and Kirschner, M. (1984). Dynamic instability of microtubule growth. Nature *312*, 237–242.

Moughamian, A.J., and Holzbaur, E.L.F. (2012). Dynactin Is Required for Transport Initiation from the Distal Axon. Neuron *74*, 331–343.

Moughamian, A.J., Osborn, G.E., Lazarus, J.E., Maday, S., and Holzbaur, E.L.F. (2013). Ordered recruitment of dynactin to the microtubule plus-end is required for efficient initiation of retrograde axonal transport. J. Neurosci. *33*, 13190–13203.

Nangaku, M., Sato-Yoshitake, R., Okada, Y., Noda, Y., Takemura, R., Yamazaki, H., and Hirokawa, N. (1994). KIF1B, a novel microtubule plus end-directed monomeric motor protein for transport of mitochondria. Cell *79*, 1209–1220.

Nassif, C., Noveen, A., and Hartenstein, V. (2003). Early development of the Drosophila brain: III. The pattern of neuropile founder tracts during the larval period. J. Comp. Neurol. *455*, 417–434.

Nguyen, L., Besson, A., Heng, J.I., Schuurmans, C., Teboul, L., Parras, C., Philpott, A., Roberts, J.M., and Guillemot, F. (2006). p27kip1 independently promotes neuronal differentiation and migration in the cerebral cortex. Genes Dev. 1511–1524.

Nichols, C.D., Becnel, J., and Pandey, U.B. (2012). Methods to Assay Drosophila Behavior. J. Vis. Exp. 3–7.

Niven, J.E., Graham, C.M., and Burrows, M. (2008). Diversity and Evolution of the Insect Ventral Nerve Cord. Annu. Rev. Entomol. *53*, 253–271.

North, B.J., and Verdin, E. (2007). Interphase nucleo-cytoplasmic shuttling and localization of SIRT2 during mitosis. PLoS One *2*.

North, B.J., Marshall, B.L., Borra, M.T., Denu, J.M., and Verdin, E. (2003). The human Sir2 ortholog, SIRT2, is

an NAD+-dependent tubulin deacetylase. Mol. Cell *11*, 437–444.

Ohkawa, N., Sugisaki, S., Tokunaga, E., Fujitani, K., Hayasaka, T., Setou, M., and Inokuchi, K. (2008). N-acetyltransferase ARD1-NAT1 regulates neuronal dendritic development. Genes to Cells *13*, 1171–1183.

Okada, Y., Yamazaki, H., Sekine-Aizawa, Y., and Hirokawa, N. (1995). The neuron-specific kinesin superfamily protein KIF1A is a unique monomeric motor for anterograde axonal transport of synaptic vesicle precursors. Cell *81*, 769–780.

Ouyang, H., Ali, Y.O., Ravichandran, M., Dong, A., Qiu, W., MacKenzie, F., Dhe-Paganon, S., Arrowsmith, C.H., and Zhai, R.G. (2012). Protein aggregates are recruited to aggresome by histone deacetylase 6 via unanchored ubiquitin C termini. J. Biol. Chem. *287*, 2317–2327.

Paschal, B.M. (1987). MAP 1C Is a Microtubule-activated ATPase Which Translocates Microtubules In Vitro and Has Dynein-l e Properties. J. Cell Biol. *105*, 1273–1282.

Paschal, B., and Vallee, R. (1987). Retrograde transport by the microtubule-associated protein MAP 1C. Nature *330*, 181–183.

Pawson, C., Eaton, B.A., and Davis, G.W. (2009). Formin-Dependent Synaptic Growth; Evidence that Dlar Signals via Diaphanous to Modulate Synaptic Actin and Dynamic Pioneer Microtubules. October *28*, 11111–11123.

Perrimon, N., Pitsouli, C., and Shilo, B.-Z. (2012). Signaling Mechanisms Controlling Cell Fate and Embryonic Patterning. Cold Spring Harb. Perspect. Biol. *4*, a005975–a005975.

Perrimon, N., Bonini, N.M., and Dhillon, P. (2016). Fruit flies on the front line: the translational impact of Drosophila. Dis. Model. Mech. *9*, 229–231.

Pfister, K.K. (2015). Distinct functional roles of cytoplasmic dynein defined by the intermediate chain isoforms. Exp. Cell Res. *334*, 54–60.

Pilling, A.D., Horiuchi, D., Lively, C.M., and Saxton, W.M. (2006). Kinesin-1 and Dynein are the primary motors for fast transport of mitochondria in Drosophila motor axons. Mol. Biol. Cell *17*, 2057–2068.

Pineda, J.R., Pardo, R., Zala, D., Yu, H., Humbert, S., and Saudou, F. (2009). Genetic and pharmacological inhibition of calcineurin corrects the BDNF transport defect in Huntington's disease. Mol. Brain *2*, 33.

Poirier, K., Lebrun, N., Broix, L., Tian, G., Saillour, Y., Boscheron, C., Parrini, E., Valence, S., Pierre, B. Saint, Oger, M., et al. (2013). Mutations in TUBG1, DYNC1H1, KIF5C and KIF2A cause malformations of cortical development and microcephaly. Nat. Genet. *45*, 639–647.

Pugacheva, E.N., Jablonski, S.A., Hartman, T.R., Henske, E.P., and Golemis, E.A. (2007). HEF1-Dependent Aurora A Activation Induces Disassembly of the Primary Cilium. Cell *129*, 1351–1363.

Reed, N.A., Cai, D., Blasius, T.L., Jih, G.T., Meyhofer, E., Gaertig, J., and Verhey, K.J. (2006). Microtubule Acetylation Promotes Kinesin-1 Binding and Transport. Curr. Biol. *16*, 2166–2172.

Reiter, L.T. (2001). A Systematic Analysis of Human Disease-Associated Gene Sequences In Drosophila melanogaster. Genome Res. *11*, 1114–1125.

Rizzuto, R., Brini, M., Pizzo, P., Murgia, M., and Pozzan, T. (1995). Chimeric green fluorescent protein as a tool for visualizing subcellular organelles in living cells. Curr. Biol. *5*, 635–642.

Roy, S. (2013). Seeing the unseen: The Hidden World of Slow Axonal Transport. Neuroscientist *20*, 71–81.

Rudolph, J.E., Kimble, M., Hoyle, H.D., Subler, M.A., and Raff, E.C. (1987). Three Drosophila beta-tubulin sequences: a developmentally regulated isoform (beta 3), the testis-specific isoform (beta 2), and an assembly-defective mutation of the testis-specific isoform (B2t8) reveal both an ancient divergence in metazoan isotypes an. Mol. Cell. Biol. *7*, 2231–2242.

Ruiz-Cañada, C., and Budnik, V. (2006). Introduction on The Use of The Drosophila Embryonic/Larval Neuromuscular Junction as A Model System to Study Synapse Development and Function, and A Brief Summary of Pathfinding and Target Recognition. Int. Rev. Neurobiol. *75*, 1–31.

Sadoul, K., and Khochbin, S. (2016). The growing landscape of tubulin acetylation: lysine 40 and many more. Biochem. J. *473*, 1859–1868.

Sanyal, S. (2009). Genomic mapping and expression patterns of C380, OK6 and D42 enhancer trap lines in the larval nervous system of Drosophila. Gene Expr. Patterns *9*, 371–380.

Saxton, W.M., and Hollenbeck, P.J. (2012). The axonal transport of mitochondria. J. Cell Sci. *125*, 2095–2104.

Schnapp, B.J., Vale, R.D., Sheetz, M., and Reese, T.S. (1985). Single Microtubules from Squid Axoplasm Support Bidirectional Movement of Organelles. Cell *40*, 455–462.

Schroer, T.A. (2004). Dynactin. Annu. Rev. Cell Dev. Biol. *20*, 759–779.

Schulze, E., Asai, D.J., Bulinski, J.C., and Kirschner, M. (1987). Posttranslational modification and microtubule stability. J. Cell Biol. *105*, 2167–2177.

Seidel, C., Schnekenburger, M., Dicato, M., and Diederich, M. (2015). Histone deacetylase 6 in health and disease. Epigenomics *7*, 103–118.

Shida, T., Cueva, J.G., Xu, Z., Goodman, M.B., and Nachury, M. V. (2010). The major α-tubulin K40 acetyltransferase αTAT1 promotes rapid ciliogenesis and efficient mechanosensation. Proc. Natl. Acad. Sci. *107*, 21517–21522.

Silverman, M.A., Kaech, S., Ramser, E.M., Lu, X., Lasarev, M.R., Nagalla, S., and Banker, G. (2010). Expression of kinesin superfamily genes in cultured hippocampal neurons. Cytoskeleton *67*, 784–795.

Sirajuddin, M., Rice, L.M., and Vale, R.D. (2014). Regulation of microtubule motors by tubulin isotypes and post-translational modifications. Nat. Cell Biol. *16*, 335–344.

Skiniotis, G., Cochran, J.C., Müller, J., Mandelkow, E., Gilbert, S.P., and Hoenger, A. (2004). Modulation of kinesin binding by the C-termini of tubulin. EMBO J. *23*, 989–999.

Solinger, J.A., Paolinelli, R., Klöß, H., Scorza, F.B., Marchesi, S., Sauder, U., Mitsushima, D., Capuani, F., Stürzenbaum, S.R., and Cassata, G. (2010a). The Caenorhabditis elegans Elongator Complex Regulates Neuronal α-tubulin Acetylation. PLoS Genet. *6*, e1000820.

Solinger, J.A., Paolinelli, R., Klöß, H., Scorza, F.B., Marchesi, S., Sauder, U., Mitsushima, D., Capuani, F., Stürzenbaum, S.R., and Cassata, G. (2010b). The Caenorhabditis elegans elongator complex regulates neuronal α-tubulin acetylation. PLoS Genet. *6*.

Song, Y., and Brady, S.T. (2015). Post-translational modifications of tubulin: Pathways to functional diversity of microtubules. Trends Cell Biol. *25*, 125–136.

St Johnston, D. (2002). The art and design of genetic screens: Drosophila melanogaster. Nat. Rev. Genet. *3*, 176–188.

Staples, J., and Broadie, K. (2013). The cell polarity scaffold Lethal Giant Larvae regulates synapse morphology and function. J. Cell Sci. *126*, 1992–2003.

Stepanova, T., Slemmer, J., Hoogenraad, C.C., Lansbergen, G., Dortland, B., De Zeeuw, C.I., Grosveld, F., van Cappellen, G., Akhmanova, A., Galjart, N., et al. (2003). Visualization of microtubule growth in cultured neurons via the use of EB3-GFP (end-binding protein 3-green fluorescent protein). J. Neurosci. *23*, 2655–2664.

Sullivan, K.F. (1988). Structure and Utilization of Tubulin Isotypes. Annu. Rev. Cell Biol. *4*, 687–716.

Szyk, A., Deaconescu, A.M., Spector, J., Goodman, B., Valenstein, M.L., Ziolkowska, N.E., Kormendi, V., Grigorieff, N., and Roll-Mecak, A. (2014). Molecular Basis for Age-Dependent Microtubule Acetylation by Tubulin Acetyltransferase. Cell *157*, 1405–1415.

Tanaka, Y., Kanai, Y., Okada, Y., Nonaka, S., Takeda, S., Harada, A., and Hirokawa, N. (1998). Targeted Disruption of Mouse Conventional Kinesin Heavy Chain kif5B, Results in Abnormal Perinuclear Clustering of Mitochondria. Cell *93*, 1147–1158.

Tazuke, S.I., Schulz, C., Gilboa, L., Fogarty, M., Mahowald, A.P., Guichet, A., Ephrussi, A., Wood, C.G., Lehmann, R., and Fuller, M.T. (2002). A germline-specific gap junction protein required for survival of differentiating early germ cells. Development *129*, 2529–2539.

Topalidou, I., Keller, C., Kalebic, N., Nguyen, K.C.Q., Somhegyi, H., Politi, K.A., Heppenstall, P., Hall, D.H., and Chalfie, M. (2012). Genetically Separable Functions of the MEC-17 Tubulin Acetyltransferase Affect Microtubule Organization. Curr. Biol. *22*, 1057–1065.

Toyoshima, H., and Hunter, T. (1994). p27, a novel inhibitor of G1 cyclin-Cdk protein kinase activity, is related to p21. Cell *78*, 67–74.

Trokter, M., Mucke, N., and Surrey, T. (2012). Reconstitution of the human cytoplasmic dynein complex. Proc. Natl. Acad. Sci. *109*, 20895–20900.

Twelvetrees, A., Hendricks, A.G., and Holzbaur, E.L.F. (2012). SnapShot: Axonal Transport. Cell *149*, 950–950.e1.

Vagnoni, A., and Bullock, S.L. (2016). A simple method for imaging axonal transport in aging neurons using the adult Drosophila wing. Nat. Protoc. *11*, 1711–1723.

Vale, R.D., Reese, T.S., and Sheetz, M.P. (1985). Identification of a novel force-generating protein, kinesin, involved in microtubule-based motility. Cell *42*, 39–50.

Vershinin, M., Carter, B.C., Razafsky, D.S., King, S.J., and Gross, S.P. (2007). Multiple-motor based transport and its regulation by Tau. Proc. Natl. Acad. Sci. U. S. A. *104*, 87–92.

Wang, Y., Fisher, J.C., Mathew, R., Ou, L., Otieno, S., Sublet, J., Xiao, L., Chen, J., Roussel, M.F., and Kriwacki, R.W. (2011). Intrinsic disorder mediates the diverse regulatory functions of the Cdk inhibitor p21. Nat. Chem. Biol. *7*, 214–221.

Webster, D.R. (1990). Detyrosination of alpha tubulin does not stabilize microtubules in vivo [published erratum appears in J Cell Biol 1990 Sep;111(3):1325-6]. J. Cell Biol. *111*, 113–122.

Webster, D.D.R., and Borisy, G.G. (1989). Microtubules are acetylated in domains that turn over slowly. J. Cell Sci. *92*, 57–65.

Wise, A., Schatoff, E., Flores, J., Hua, S.-Y., Ueda, A., Wu, C.-F., and Venkatesh, T. (2013). Drosophila-Cdh1 (Rap/Fzr) a regulatory subunit of APC/C is required for synaptic morphology, synaptic transmission and locomotion. Int. J. Dev. Neurosci. *31*, 624–633.

Wise, A., Tenezaca, L., Fernandez, R.W., Schatoff, E., Flores, J., Ueda, A., Zhong, X., Wu, C.-F., Simon, A.F., and Venkatesh, T. (2015). Drosophila mutants of the autism candidate gene neurobeachin (rugose) exhibit neuro-developmental disorders, aberrant synaptic properties, altered locomotion, and impaired adult social behavior and activity patterns. J. Neurogenet. *29*, 135–143.

Wu, J.S., and Luo, L. (2006). A protocol for dissecting Drosophila melanogaster brains for live imaging or immunostaining. Nat. Protoc. *1*, 2110–2115.

Xiong, Y., Zhao, K., Wu, J., Xu, Z., Jin, S., and Zhang, Y.Q. (2013). HDAC6 mutations rescue human tau-induced microtubule defects in Drosophila. Proc. Natl. Acad. Sci. *110*, 4604–4609.

Yajima, H., Ogura, T., Nitta, R., Okada, Y., Sato, C., and Hirokawa, N. (2012). Conformational changes in tubulin in GMPCPP and GDP-taxol microtubules observed by cryoelectron microscopy. J. Cell Biol. *198*, 315–322.

Yoon, M.-K., Mitrea, D.M., Ou, L., and Kriwacki, R.W. (2012). Cell cycle regulation by the intrinsically disordered proteins p21 and p27. Biochem. Soc. Trans. *40*, 981–988.

Zala, D., Hinckelmann, M., Yu, H., Menezes, M., Cordelières, F.P., Marco, S., and Saudou, F. (2013). Vesicular Glycolysis Provides On-Board Energy for Fast Axonal Transport. Cell *152*, 479–491.

Zhang, Y., Li, N., Caron, C., Matthias, G., Hess, D., Khochbin, S., and Matthias, P. (2003). HDAC-6 interacts with and deacetylates tubulin and microtubules in vivo. EMBO J. *22*, 1168–1179.

Zhang, Y.Q., Rodesch, C.K., and Broadie, K. (2002). Living synaptic vesicle marker: synaptotagmin-GFP. Genesis *34*, 142–145.

Zhou, S.-F., Li, J.-P., Yang, Y.-X., Liu, Q.-L., Pan, S., He, Z., Zhang, X., Yang, T., Chen, X.-W., Wang, D., et al. (2015). The investigational Aurora kinase A inhibitor alisertib (MLN8237) induces cell cycle G2/M arrest, apoptosis, and autophagy via p38 MAPK and Akt/mTOR signaling pathways in human breast cancer cells. Drug Des. Devel. Ther. 1627.